Harmful Algae 148 (2025) 102908

Contents lists available at ScienceDirect

Harmful Algae

journal homepage: www.elsevier.com/locate/hal

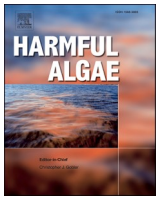

Ocean acidification changes the interspecific competition of *Sargassum fusiforme* and *Ulva lactuca* by regulating carbon and nitrogen metabolism

Cong Cao [a,#], Dongya Bao [a,#], Lili Xu [a], Zengling Ma [a,d], Mingjiang Wu [a,d], Guang Gao [b], Kit Wayne Chew [c], Shuaipeng Tian [a], Binbin Chen [a,d,*]

[a] National and Local Joint Engineering Research Center of Ecological Treatment Technology for Urban Water Pollution, Wenzhou University, Wenzhou 325035, China
[b] State Key Laboratory of Marine Environmental Science, College of Ocean and Earth Sciences, Xiamen University, Xiamen 361005, China
[c] School of Chemistry, Chemical Engineering and Biotechnology, Nanyang Technological University, Singapore 637459, Singapore
[d] Zhejiang Provincial Key Lab for Subtropical Water Environment and Marine Biological Resources Protection, Wenzhou University, Wenzhou 325035, China

ARTICLE INFO

Keywords:
Interspecific competition
Climate change
Ecophysiology
Macroalgae
Ocean acidification

ABSTRACT

Due to different response mechanisms of cultivated *Sargassum fusiforme* and its main epiphyte *Ulva lactuca* to ocean acidification caused by increased CO_2 concentrations, the effects of *U. lactuca* on its host may be different at elevated CO_2 concentrations. In this study, the effects of *U. lactuca* on the photosynthetic carbon assimilation process of *S. fusiforme* were studied under the condition of elevated CO_2 concentration. The results showed that co-culture with *U. lactuca* significantly inhibited the growth, photosynthesis and nitrogen metabolism of *S. fusiforme*, up-regulated the expression of its carbon assimilation-related genes such as antenna protein, phosphoglycerate kinase (PGK), ribulose-1,5-diphosphate carboxylase/oxygenase (RuBisCo), and down-regulated the expression of genes associated with growth and nitrogen metabolism. Under monoculture conditions, the growth and photosynthesis of *S. fusiforme* were significantly enhanced by elevated CO_2, and the expressions of photosynthetic carbon assimilation and antenna protein-related genes were up-regulated, reflecting the promotion of *S. fusiforme* photosynthesis. However, the enzyme activity and gene expression of nitrogen metabolism were inhibited. Under co-culture condition, the increase of CO_2 concentration also promoted the photosynthesis and growth of *S. fusiforme*, and up-regulated the expression of genes related to photosystem II (PSII) central proteins (including D1 and D2 proteins). The results of this study showed that *U. lactuca* inhibited the photosynthesis, growth and nitrogen metabolism of *S. fusiforme*, while ocean acidification promoted the photosynthesis of *S. fusiforme* by increasing activity of PSII, changing the carbon and nitrogen metabolism strategy, thus greatly alleviating the interspecific stress from its epiphyte *U. lactuca*. These results had important implications for exploring the ecological significance of seaweed farming and carbon sequestration efficiency in the context of future climate change.

1. Introduction

Sargassum fusiforme (Harv.) Setchell is an economically important seaweed that is widely cultivated in the coastal areas of China and South Korea (Kokubu et al., 2015; Sun et al., 2019; Zhang et al., 2020a) because of its high medicinal and edible values (Chen et al., 2012; Jia et al., 2020; Liu et al., 2020; Zhang et al., 2020a). Large-scale cultivation of offshore macroalgae, in addition to promoting local economic development, can also effectively alleviate eutrophication, increase marine carbon sequestration, and achieve carbon neutralization in coastal waters (Hartmann et al., 2013; Froehlich et al., 2019; Zemah--Shamir et al., 2021).

In the context of climate change, the proliferation of epiphytic algae has become a serious obstacle to large-scale seaweed cultivation. Epiphytic algae compete with the host throughout the culture phase (Garcia-Redondo et al., 2019; Chen et al., 2022; Tian et al., 2022a; 2022b; Xu et al., 2022). They also interact with economic seaweed by consuming limited resources. For example, the rapid growth of epiphytic algae reduces the concentration of dissolved inorganic carbon (DIC) in economic seaweed culture zones, thus inhibiting host growth and

* Corresponding author.
E-mail address: binbch@163.com (B. Chen).
# C Cao and D Bao contributed equally to this work and should be regarded as co-first authors.

https://doi.org/10.1016/j.hal.2025.102908
Received 25 June 2024; Received in revised form 27 January 2025; Accepted 27 May 2025
Available online 5 June 2025

photosynthesis (Friedlander, 1992; Chen and Zou, 2015; De et al., 2019; Gao et al., 2019). Epiphytic algae can directly affect cultured seaweed through allelopathy (Chen et al., 2019a; Shang et al., 2020), or reduce photosynthetic activity of economic algae by shading (Baer and Stengel, 2014).

In recent years, the ocean's absorption of large amount of anthropogenic CO_2 has led to a decrease surface water pH of 0.1–0.2 unit, leading to ocean acidification (Doney et al., 2009; Gattuso et al., 2015; Peña et al., 2021). At high concentrations of CO_2, the surface seawater carbonate system changes, with increased concentrations of CO_2 and HCO_3^- and decreased concentration of CO_3^{2-} (Key et al., 2005). These changes affect algal photosynthesis, carbon assimilation, inorganic salt ions utilization, and algae growth (Albert et al., 2020; Zhang et al., 2020b; Barakat et al., 2021; Liu et al., 2021; Wen and Zou, 2021). However, at high CO_2 concentration, physiological metabolic processes such as algae photosynthesis have different responses to the decrease of seawater pH value and the change of carbonate system (Chen and Zou, 2015; Ayache et al., 2021; Liu et al., 2021; Wei et al., 2021). Previous results have shown that economic and epiphytic algae respond differently to increased CO_2 concentration. For example, elevated CO_2 concentration can enhance the growth of *Gracilaria lemaneiformis*, reinforce nutrient uptake, and influence photosynthesis (Xu et al., 2008). Similarly, previous studies have shown that increasing CO_2 concentration can significantly promote the growth of *S. fusiforme* (Zou, 2005; Chen et al., 2019b). However, high CO_2 concentration had no significant effect on the growth of *Ulva* L. (Axelsson et al., 1999; Kang and Kim, 2016; Kang and Chunget, 2017; Ji et al., 2019), since these algae may have efficient CO_2 concentrations mechanisms, their photosynthetic rates may become saturated at current CO_2 level. As a result, macroalgae may respond differently to CO_2 concentrations, thereby affecting the efficiency changes of photosynthetic carbon assimilation, which in turn affects the supply of carbon sources in photosynthesis. Additionally, Stitt and Krapp (1999) demonstrated that changes in CO_2 concentration can affect the activity of many key enzymes in nitrogen metabolism, and the absorption rate of NO_3^- by macroalgae is related to the activity of nitrate reductase (NR) (Gao et al., 1993). At the same time, the absorption and assimilation of nitrogen sources will also be affected. For example, excessive carbon sources and a deficiency of nitrogen sources may lead to the accumulation and storage of photosynthetic products, such as mannitol (Raven and Hurd, 2012).

Ocean acidification also affect the interspecific competition of macroalgae. Co-culture with epiphytic *U. lactuca* inhibited the photosynthesis and growth of *Gracilaria lemaneiformis*, and the inhibition was more significant under high CO_2 conditions (Chen et al., 2015). In addition, at high concentrations of CO_2, *U. lactuca* produced secondary metabolite dimethyl sulfonyl propionic acid (DMSP) (Kerrison et al., 2012). DMSP destroyed the cell membrane of *Neoporphyra haitanensis* and decreased the resistance of the latter. It can also negatively affect photosynthesis and nitrogen metabolism in algal cells, affecting algal growth (Chen et al., 2019a). Brown algae *S. fusiforme* and red algae have different structural characteristics and physiological metabolic mechanism. In addition, the effects of epiphytic algae on the growth and physiological metabolism of cultured algae also changed under high CO_2 concentration. Thus, *S. fusiforme* may respond to the combined effects of epiphytes and ocean acidification.

During marine cultivation, *U. lactuca* not only attached to *S. fusiforme*, but also more commonly found on the seedling ropes. As a dominant epiphytic algal species on economic seaweeds, *U. lactuca* has a strong photosynthetic and nutrient absorption capacity (Tian et al., 2022b). Therefore, these epiphytic algae grow rapidly, occupy the space of the host, and form interspecific competition. Whether epiphytic algae competed with economic seaweed for nutrients from the environment, or exert influence on the growth and nutritional quality of economic seaweed through shading and/or allelopathy, the economic benefits and carbon sequestration of cultured seaweed will be affected, so it is necessary to further study and elaborate its physiological response mechanism. Therefore, in the context of the current intensified climate change caused by the increase of CO_2 concentration, it is of great importance to explore the changes in the interspecific competition mechanism of macroalgae, especially economic seaweed, under ocean acidification for the study of future marine carbon sequestration benefits (Behrenfeld et al., 2002; Hill et al.2015., 2015; Krause-Jensen et al., 2016). In this study, the influence mechanisms of *U. lactuca* on the photosynthetic carbon assimilation of *S. fusiforme* and its changes under high CO_2 concentration were studied by using monoculture and co-culture experiments. The aims of this study were to analyze the response mechanisms of *S. fusiforme* under high CO_2 concentration and epiphytic algae stress, and to provide theoretical basis for *S. fusiforme* cultivation to cope with ocean acidification and interspecific competition.

2. Materials and methods

2.1. Sample collection and experimental treatments

S. fusiforme and *U. lactuca* were collected in *S. fusiforme* cultivation area in Dongtou, Zhejiang Province and transferred to the laboratory in a low-temperature foam box (about 4 °C). The samples were cleaned with filtered and sterilized natural seawater to remove the attached organisms and impurities on the surface. Due to the morphological and structural differences between *S. fusiforme* and *U. lactuca* (Lin et al., 2020; Dominguez and Loret, 2019), the cultivation densities of *S. fusiforme* (S) and *U. lactuca* (U) were set at 10 g L^{-1} and 3 g L^{-1}, respectively, during single-species cultivation (M), while during mixed cultivation (B), they were set at 5 g L^{-1} and 1.5 g L^{-1}, respectively (Cao et al., 2022). Healthy algae were selected based on the above-mentioned culture density and pre-cultured separately for 2 days in a CO_2 plant incubator (Percival E-36HO, America), illuminated by fluorescent tubes with an intensity of 100 μmol photons $m^{-2}{\cdot}s^{-1}$ (L:D = 12 h:12 h), and maintained at a temperature of 19(±1) °C. Sterilized natural seawater with a salinity of 29 ‰ was supplemented with $NaNO_3$ solution and $Na_2HPO_4{\cdot}2H_2O$ solution until the final concentrations were 200 μmol L^{-1} and 20 μmol L^{-1}, respectively, and continuously aerated with ambient air.

For the experiments, the CO_2 concentration of the CO_2 plant incubator was adjusted to ambient CO_2 concentration of 430 ppm (A) and elevated CO_2 concentration of 1000 ppm (E), respectively. Therefore, the treatment groups were SMA (*S. fusiforme* grown at monoculture and ambient CO_2 concentration); SME (*S. fusiforme* grown at monoculture and elevated CO_2 concentration); SBA (*S. fusiforme* grown at co-culture and ambient CO_2 concentration); SBE (*S. fusiforme* grown at co-culture and elevated CO_2 concentration); UMA (*U. lactuca* grown at monoculture and ambient CO_2 concentration); UME (*U. lactuca* grown at monoculture and elevated CO_2 concentration); UBA (*U. lactuca* grown at co-culture and ambient CO_2 concentration); UBE (*U. lactuca* grown at co-culture and elevated CO_2 concentration) . Each treatment group included three replicate cultures. The culture medium was refreshed every 3 days, with $NaNO_3$ solution and $Na_2HPO_4{\cdot}2H_2O$ solutions re-added as required. All other conditions remained consistent with those during the pre-culture phase. Physiological indices and transcriptomic analysis were assessed after 4 weeks of culture.

Seawater carbonate systems for different treatment conditions were also analyzed. The total alkalinity (TA) was determined using the classical Gran electrical method (Gran, 1952). The concentrations of total DIC, CO_3^{2-} and HCO_3^- were then estimated based on pCO_2, pH, and total alkalinity by using the CO_2SYS software program (Lewis and Wallace, 1998).

2.2. Growth determination

The determination of relative growth rate (RGR) refers to the method of Yong et al. (2013). The initial fresh weight (W_0) and fresh weight after

t days (W_t) of the cultured algae were measured, and RGR of *S. fusiforme* and *U. lactuca* were all calculated using the following formula: RGR (% day^{-1}) = [(W_t / W_0)$^{1/t}$ - 1] × 100 %, where t (day) is the cultivation time.

2.3. Analysis of photosynthetic characteristics

The relative electron transfer rate (rETR) of *S. fusiforme* and *U. lactuca* were measured using a pulse-amplitude modulated fluorometer (Junior-PAM; Walz, Effeltrich, Germany). Chlorophyll fluorescence parameters were obtained by measuring the leaves of *S. fusiforme* and *U. lactuca* at 10:00 am. Each sample was adapted to dark conditions for 20 min. The algae leaves were firstly clamped with a magnetic clip that comes with Junior-PAM. Eleven actinic lights within the range of 0–820 μmol photons $m^{-2}{\cdot}s^{-1}$ were selected to measure rETR (Xu et al., 2022; Luo et al., 2023). A sample was illuminated at each light intensity for 10 s prior to firing a saturating pulse. The RLCs were fitted according to Platt's formula (Platt et al., 1980):

$$rETR = rETRm{\cdot}\left(1 - e^{-\alpha \cdot PAR/rETRm}\right){\cdot}e^{-\beta \cdot PAR/rETRm}$$

where α is the initial slope, which reflects the utilization efficiency of light energy, and β is the light suppression parameter.

The maximum quantum yield (*Fv/Fm*) of PSII was measured, where $Fv = Fm - F_0$, *Fm* is the maximum fluorescence after dark adaptation, and F_0 is the minimum fluorescence after dark adaptation for 20 min. Non-photochemical quenching (NPQ) was measured by the formula: NPQ = (*Fm - Fm'*) / *Fm'*, where *Fm'* is the maximum fluorescence under light adaptation (Genty et al., 1989).

Algal discs were cut into small sections (1–2 cm) using a sterile blade and incubated in seawater for at least 2 h under the same culture conditions and light exposure. This pretreatment was conducted to minimize the potential impact of cutting-induced cell damage on subsequent respiratory or photosynthetic measurements. Then, approximately 0.2 g (Fw) of *S. fusiforme* was added to a chamber containing 20 mL of the original culture medium that was magnetically stirred. A liquid phase oxygen electrode (YSI Model 5300; Yellow Springs Instrument Co., OH, USA) was used to measure changes in the oxygen content in the reaction chamber and calculated the maximum net photosynthetic rate (Pm) and dark respiration rate (Rd). The Pm was measured at a light intensity of 400 μmol photons $m^{-2}{\cdot}s^{-1}$ provided by halogen lamp by adjusting the distance between the lamp source and reaction chamber. The Rd was measured at darkness. All samples were adapted to each light intensity for 6 min. Pm and Rd were expressed in μmol $O_2{\cdot}g^{-1}$ $Fw{\cdot}h^{-1}$ (Xu et al., 2022; Luo et al., 2023), and each treatment was repeated three times. Intact *S. fusiforme* algae were collected after the physiological experiments, and the attachments were washed off with sterilized seawater. The samples were rapidly frozen in liquid nitrogen and stored at −80 °C for subsequent comparative transcriptome analysis and qPCR validation.

2.4. Mannitol content determination

The determination of mannitol content refers to the method of Lin et al. (2014) with minor modification. Fresh and healthy algae with no attachment of miscellaneous algae on the surface were dried at 100℃ for 30 min, then dried at 65℃ to constant weight. The dried sample was ground and submerged in 30 mL of 1 % hydrochloric acid for 4 min stirring under 100℃ water bath conditions. Then it was centrifuged at 5000 rpm for 5 min. 1 mL of the supernatant was added with 1 mL of sodium periodate solution. After 15 min of standing, 2 mL of 0.1 % rhamnose solution was added for 1 min reaction. Then 4 mL of Nash reagent was added and the reaction system was heated in a 53 ℃ constant temperature water bath for 15 min. After cooling to room temperature, the absorption value at 413 nm wavelength was measured and standardized with distilled water.

2.5. Pigments content determination

A sample of 0.1 g was weighed and homogenised in 100 % methanol. The homogenate was incubated at 4 °C for 12 h, and later centrifuged at 5000 rpm for 10 min at 4 °C. The supernatant was used to determine the contents of Chlorophyll *a* (Chl *a*), Chlorophyll *c* (Chl *c*) and carotenoids (Car) according to the methods of Porra (2002) and Parsons (1963) by using spectrophotometer (UV-1800; Shimadzu, Kyoto, Japan). The pigments were all expressed in $mg{\cdot}g^{-1}$.

2.6. Estimation of enzyme activity related to nitrogen metabolism

Nitrate reductase (NR) activity was estimated according to the method described by Corzo and Niell (1991). Approximately 0.1 g of *S. fusiforme* was placed in 10 mL of incubation medium, which contained 0.1 $mol{\cdot}L^{-1}$ KH_2PO_4, 0.5 $mmol{\cdot}L^{-1}$ Na-EDTA, 50 $mmol{\cdot}L^{-1}$ KNO_3, and 0.01 $mmol{\cdot}L^{-1}$ glucose. The sample was then flushed with N_2 gas for 30 min followed by incubation at 30 ℃ and in the dark for 30 min. Next, 2 mL of the supernatant was transferred to a colorimetric tube and 1 mL of sulfonamide reagent and 1 mL of naphthalene ethylenediamine hydrochloride reagent were added. After incubation for 15 min, the content of NO_2^--N in the sample was measured with a UV spectrophotometer (UV-1800, Shimadzu, Kyoto, Japan) at 543 nm wavelength. NR activity was expressed in μmol $NO_2^-{\cdot}g^{-1}{\cdot}h^{-1}$.

The enzyme activities of glutamate synthase (GOGAT) and glutamine synthetase (GS) were measured following the manufacturer's protocol for the commercial enzyme activity detection kit (Comin Biotechnology Co., Ltd., Suzhou, China), respectively.

2.7. Comparative transcriptome analysis

Total RNA was extracted from the frozen *S. fusiforme* by using a total RNA isolation kit (Biomarker, China). The RNA integrity and concentration were determined, and a cDNA library was constructed. The Illumina HiSeq high-throughput sequencing platform was used to sequence the cDNA to generate a large amount of high-quality raw data. Then removed the joint sequences and low-quality reads to obtain high-quality clean data. A clean data sequence was assembled to obtain the unigenes library for this species. To analyze the mechanisms underlying the influences of high CO_2 concentration and *U. lactuca* on the growth and photosynthetic carbon assimilation of *S. fusiforme*, it was necessary to analyze the metabolic pathways of differential gene enrichment. To eliminate genetic variability between individuals, biological replication was required, and Pearson correlation coefficient R was used to analyze the correlation between replications (Schulze et al., 2012).

The unigenes sequence was checking using the databases of non-redundant protein sequences (NR), Swiss-Pro, Gene Ontology (GO), Cluster of Orthologous Groups (COG), EuKaryotic Orthologous Groups (KOG), eggNOG, and KEGG (Kyoto Encyclopedia of Genes and Genomes) by using BLAST software (He et al., 2018), and the unigene annotation information was obtained to systematically analyze the metabolic pathways and functions of gene products. Fragments per kilobase of transcript per million mapped reads (FPKM) is also commonly used for estimating gene expression levels in transcriptome sequencing data analysis (Mortazavi et al., 2008).

The Benjamini-Hochberg method was used to correct the *p* value obtained from the original hypothesis test, and the corrected *p* value, namely the error rate (FDR), was considered as the key to screen differentially expressed genes (DEGs) (Benjamini and Hochberg, 1995). In this experiment, the DEGs were screened with FDR < 0.01 and | log 2 (fold change) | value; | log 2 (fold change) | ≥ 1 was up-regulated, and | log 2 (fold change) | ≤ −1 was down-regulated. The FPKM values were used to express the content of fucoxanthin-chlorophyll proteins (FCPs) in *S. fusiforme* under different treatment conditions.

2.8. Real-time quantitative reverse transcription polymerase chain reaction (qRT-PCR) analysis

Primer Premier 5 software was used for primer design. The product was controlled to about 100 bp, and the Tm value was controlled at 60–63 °C (Table S1). Six target genes were selected for the qRT-PCR analysis: glutathione peroxidase (*GSH-Px*), 6-phosphogluconate dehydrogenase (*6-PGDH*), light harvesting complex protein (*LHC*), ribulose phosphate epimerase (*RPE*), glutathione S-transferase (*GST*), glutamate cysteine ligase (*GCL*), and the internal reference gene (actin) (Table S2). *GSH-Px* is an important peroxidase decomposition enzyme widely existing in organism, which promotes the decomposition of H_2O_2 to protect the structure and function of cell membrane from the interference and damage of oxide (Panday et al., 2020). *6-PGDH* is an important enzyme in pentose phosphate pathway, which can be used to synthesize many reducing agents (Hanau and Helliwell, 2020). *LHC* is major component of the PSI light harvesting antenna (Chukhutsina et al., 2020). *RPE* catalyzing the reversible interconversion of d-xylulose 5-phosphate and its epimer, d-ribulose 5-phosphate (Liang et al., 2011). *GST* has the function of repairing oxidized macromolecules such as DNA and protein (Vaish et al., 2020). *GCL* is the rate-limiting enzyme of glutathione synthesis (Okada and Kimura, 2022). These genes were selected their significant differences in the comparative transcriptome under the treatments, which were further verified after screening in combination with photosynthesis. All reactions were performed using a qRT-PCR system, and $2^{-\Delta\Delta t}$ method was used to calculate gene expression (Livak and Schmittgen, 2001).

2.9. Statistical analyses

Physical and chemical parameter data were calculated and processed using Excel (Microsoft, USA), and statistical analysis, including two-way ANOVA and *t*-test, the experimental results were performed using SPSS 25.0 (Amonk, NY, USA). Origin 2017 (Origin, USA) was used for plotting, and the experimental results were expressed as mean ± standard deviation (mean ± SD). For the transcriptome analysis, SPSS (version 25.0, Amonk, NY, USA) was used to perform one-way analysis of variance of the experimental results, and Graphpad prism (version 10, San Diego, California, USA) was used for plotting. The gene expression level was expressed as mean ± SD, and the significance level was set at $p < 0.05$ and the extremely significance level was $p < 0.01$. The FPKM method was used to calculate the expression of protein-coding genes and screen differentially expressed genes at $p < 0.05$; $|\log 2 \text{ foldchange}| \geq 1$ was used to create a differential gene expression volcano map.

3. Results

3.1. Changes in seawater carbonate system

The elevated CO_2 concentration outstandingly altered the carbonate system of seawater (Table 1). Compared to ambient CO_2 conditions, elevated CO_2 concentrations reduced the pH levels of both monoculture and co-culture seawater by 3.74 % and 5.08 %, respectively ($p < 0.01$). Additionally, under high CO_2 conditions, the CO_2 concentrations in monoculture and co-culture increased by 147.20 % and 223.02 %, respectively ($p < 0.01$), while bicarbonate (HCO_3^-) concentrations rose by 21.05 % and 22.86 %, respectively ($p < 0.01$). Conversely, carbonate (CO_3^{2-}) concentrations decreased by 40.71 % and 53.29 %, respectively ($p < 0.01$). Notably, under ambient CO_2 conditions, co-culture (SBA) had no significant effect on the seawater carbonate system. In contrast, cultivation methods involving elevated CO_2 concentrations, such as monoculture under elevated CO_2 (SME) and co-culture under elevated CO_2 (SBE), significantly altered the seawater carbonate parameters compared to monoculture under ambient CO_2 conditions (SMA).

3.2. RGR of S. fusiforme and U. lactuca

Fig. 1a presents the morphological changes in *S. fusiforme* from the early stage to the end of culture. Under the ambient CO_2 concentration, the RGR of *S. fusiforme* was significantly lower in co-culture compared to monoculture ($p < 0.05$). In monoculture, elevated CO_2 concentration significantly promoted the RGR of *S. fusiforme* ($p < 0.05$). However, under elevated CO_2 concentration with co-culture, the RGR of *S. fusiforme* was significantly lower than that observed in monoculture under ambient CO_2 concentration ($p < 0.05$), but there was no significant difference compared to co-culture under ambient CO_2 concentration ($p > 0.05$) (Fig. 1b). In addition, the RGR of *U. lactuca* in co-culture was significantly lower than in monoculture ($p < 0.05$); Under elevated CO_2 concentration, *U. lactuca* exhibited no significant difference of the RGR between the conditions of co-culture and monoculture ($p > 0.05$) (Fig. 1c).

3.3. Photosynthetic characteristics of S. fusiforme and U. lactuca

The RLCs of *S. fusiforme* and *U. lactuca* were affected by the CO_2 concentration and co-culture (Fig. 2). In monoculture, the rETRs of *S. fusiforme* increased significantly under high CO_2 concentration. When *S. fusiforme* was co-cultured with *U. lactuca*, the rETRs of *S. fusiforme* at ambient CO_2 concentration were lower than that at high CO_2 concentration (Fig. 2a). Under co-cultured conditions, the rETRs of *U. lactuca* under high CO_2 concentration were higher than under other treatment (Fig. 2b). The Pm was significantly affected by the treatment of high CO_2 concentration and co-culture (Table 2). In monoculture, Pm of *S. fusiforme* under high CO_2 concentration was significantly higher than under ambient CO_2 concentration ($p < 0.05$). In co-culture, Rd of *S. fusiforme* was the highest under ambient CO_2 concentration ($p < 0.05$) (Fig. 2c). In monoculture, Pm of *U. lactuca* under high CO_2 concentration was significantly higher than that under ambient CO_2 concentration ($p < 0.05$). Meanwhile, in monoculture, Rd of *U. lactuca* under high CO_2 concentration was significantly higher than that under the other treatment groups ($p < 0.05$) (Fig. 2d).

Under ambient CO_2 concentration, the rETRm value of *S. fusiforme* in co-culture was significantly lower than in monoculture ($p > 0.05$), whereas the *Fv/Fm* ($p = 0.2$) and α ($p = 0.065$) of *S. fusiforme* in co-culture were not significantly different from those in monoculture (Fig. 3a, b, c). In monoculture, rETRm, *Fv/Fm*, and α of *S. fusiforme*

Table 1
Parameters of seawater carbonate system under different treatment groups. Different lowercase letters represent significant differences. Data are the means ± SD ($n = 3$).

Treatment	CO_2 levels (ppm)	pH	TA (μmol kg^{-1})	CO_2 (μmol kg^{-1})	CO_3^{2-} (μmol kg^{-1})	HCO_3^- (μmol kg^{-1})	DIC (μmol kg^{-1})
SMA	430	8.27 ± 0.1^a	2682.08 ± 10.10^c	8.92 ± 0.03^c	286.16 ± 1.19^a	2009.85 ± 7.86^c	2304.93 ± 9.01^c
SME	1000	7.86 ± 0.1^b	2828.60 ± 21.82^a	28.15 ± 0.22^b	141.96 ± 1.14^c	2496.32 ± 19.59^a	2666.45 ± 20.92^a
SBA	430	8.26 ± 0.1^a	2664.23 ± 6.08^c	9.12 ± 0.02^c	279.31 ± 0.66^b	2007.41 ± 4.76^c	2295.83 ± 5.44^c
SBE	1000	7.84 ± 0.1^b	2771.63 ± 20.47^b	29.46 ± 0.22^a	130.47 ± 0.98^d	2466.37 ± 18.51^b	2626.30 ± 19.71^b

Notes: TA, total alkalinity; DIC, dissolved inorganic carbon; SMA, *S. fusiforme* grown at monoculture and ambient CO_2 concentration; SME, *S. fusiforme* grown at monoculture and elevated CO_2 concentration; SBA, *S. fusiforme* grown at co-culture and ambient CO_2 concentration; SBE, *S. fusiforme* grown at co-culture and elevated CO_2 concentration.

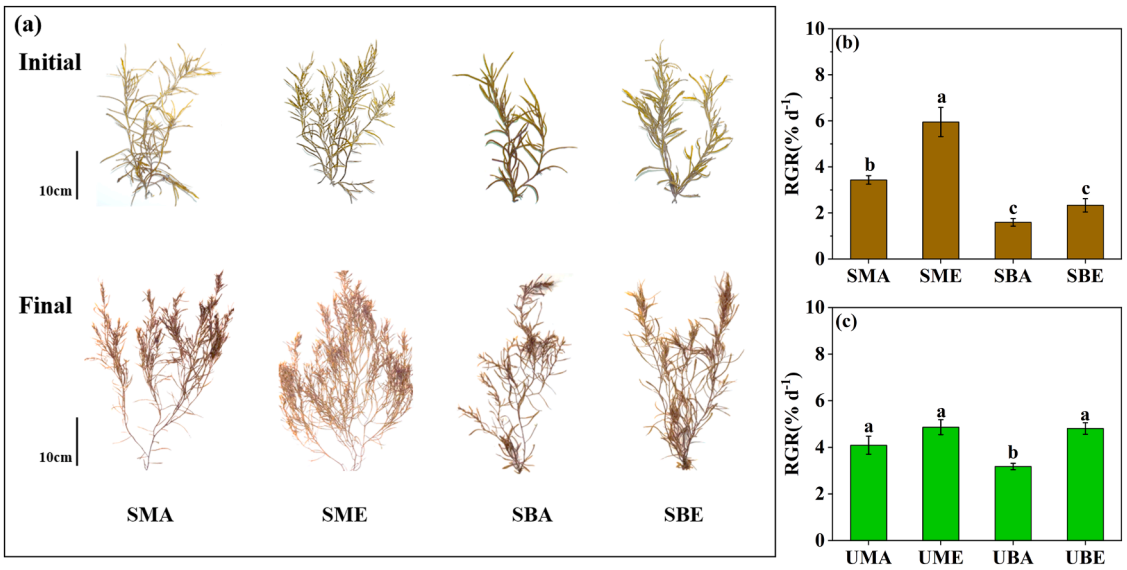

Fig. 1. Morphological changes in *Sargassum fusiforme* (a), and the relative growth rate (RGR) of *S. fusiforme* (b) and *Ulva lactuca* (c) under different treatment conditions. Different lowercase letters represent significant differences. Values represent means ± SD ($n = 3$). (SMA: *S. fusiforme* grown at monoculture and ambient CO_2 concentration; SME: *S. fusiforme* grown at monoculture and elevated CO_2 concentration; SBA: *S. fusiforme* grown at co-culture and ambient CO_2 concentration; SBE: *S. fusiforme* grown at co-culture and elevated CO_2 concentration; UMA: *U. lactuca* grown at monoculture and ambient CO_2 concentration; UME: *U. lactuca* grown at monoculture and elevated CO_2 concentration; UBA: *U. lactuca* grown at co-culture and ambient CO_2 concentration; UBE: *U. lactuca* grown at co-culture and elevated CO_2 concentration).

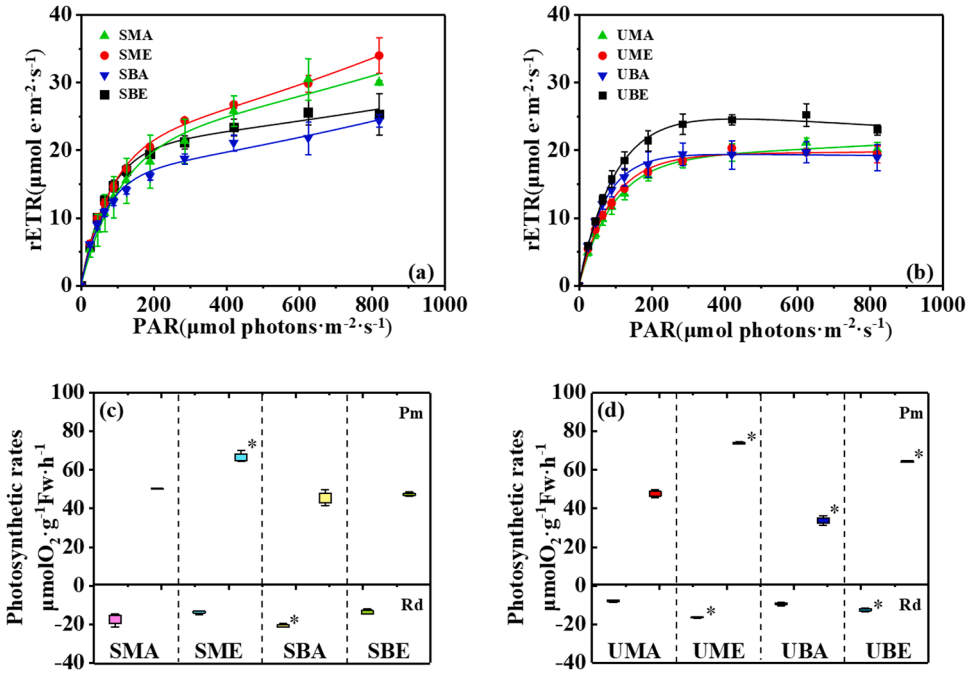

Fig. 2. Rapid light curves (RLCs) of *Sargassum fusiforme* (a) and *Ulva lactuca* (b) under different treatment conditions, and their maximum net photosynthetic rate (Pm) and dark respiration rate (Rd) (c, d). * Represent there was a statistical difference (*: $p < 0.05$; **: $p < 0.01$). Values represent means ± SD ($n = 3$).

grown at high CO_2 concentration were all significantly higher than those under ambient CO_2 ($p < 0.05$). Moreover, the rETRm of *S. fusiforme* grown at coupling conditions of high level of CO_2 and co-culture was significantly lower than in monoculture at ambient CO_2 ($p < 0.01$) (Fig. 3a).

Under ambient CO_2 concentration, no significant differences in rETRm of *U. lactuca* were observed between in co-culture and monoculture ($p > 0.05$), but *Fv/Fm* ($p < 0.05$) and α ($p < 0.05$) of *U. lactuca* grown at co-culture were significantly higher than monoculture (Fig. 3d, e, f). Under high CO_2 concentration, the rETRm of *U. lactuca* grown at co-culture was significantly higher than that at the treatment of monoculture and ambient CO_2 concentration ($p < 0.01$) (Fig. 3d). The results of the two-way ANOVA indicated that CO_2 concentrations and culture ways had significant interaction with the rETRm of *U. lactuca* (Table 2).

Under ambient CO_2 concentration, the NPQ of *S. fusiforme* in co-culture was significantly lower than the value in monoculture ($p < 0.05$) (Fig. 4a). However, under monoculture conditions, elevated CO_2 slightly increased the NPQ of *S. fusiforme* (Fig. 4a).

Table 2
Results of two-way ANOVA for maximum net photosynthetic rate (Pm), dark respiration rate (Rd), photosynthetic parameters in monoculture or co-culture of *Sargassum fusiforme* and *Ulva lactuca* under ambient CO_2 or elevated CO_2 treatments.

	S. fusiforme				*U. lactuca*			
Treatment	DF	MS	F-value	P-value	DF	MS	F-value	P-value
Pm								
CO_2 level	1	175.398	13.854	0.02	1	2416.583	823.258	<0.001
Cultivation way	1	297.97	23.535	0.008	1	414.609	141.245	<0.001
Cultivation way×CO_2 level	1	114.572	9.05	0.04	1	13.522	4.607	0.064
Rd								
CO_2 level	1	16.441	15.058	0.79	1	100.939	186.176	<0.001
Cultivation way	1	27.244	24.053	0.862	1	5.043	9.302	0.016
Cultivation way×CO_2 level	1	9.957	9.119	0.695	1	21.048	38.823	<0.001
rETRm								
CO_2 level	1	58.578	94.935	<0.001	1	8.747	8.744	0.018
Cultivation way	1	114.571	185.681	<0.001	1	19.449	19.443	0.002
Cultivation way×CO_2 level	1	14.29	23.159	0.001334	1	133.874	13.87	0.006
α								
CO_2 level	1	0.0002	3.179	0.002	1	0.006	65.663	0.00004
Cultivation way	1	0.002	20.275	0.112	1	0.002	21.801	0.002
Cultivation way×CO_2 level	1	0.0002	2.375	0.162	1	0.00003	0.328	0.583
Fv/Fm								
CO_2 level	1	0.003	7.371	0.26	1	0.02	187.285	<0.001
Cultivation way	1	0.003	7.067	0.29	1	0.005	47.975	0.0001
Cultivation way×CO_2 level	1	0.000001	0.003	0.956	1	0.001	5.245	0.051

Notes: rETRm, the maximum relative electron transfer rate; Fv/Fm, the maximum quantum yield; α, apparent photosynthetic efficiency.

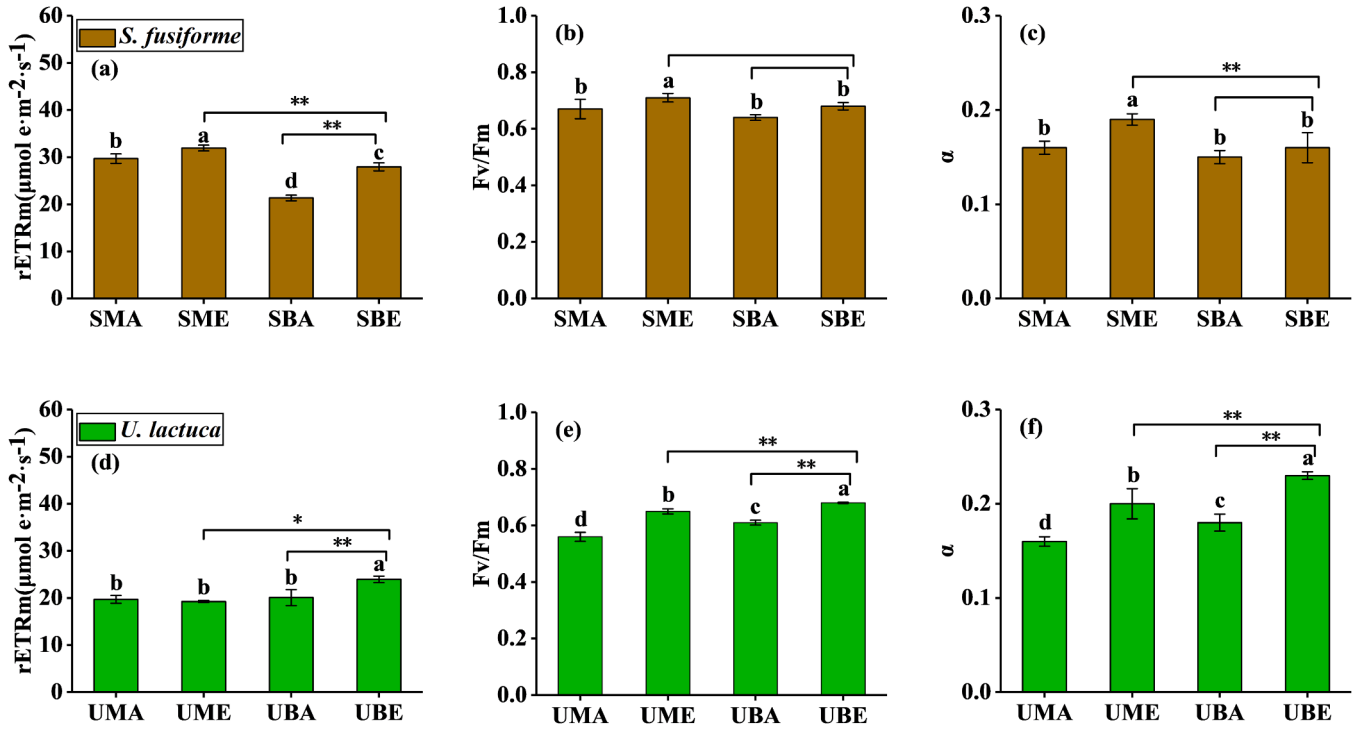

Fig. 3. The maximum electron transfer rate (rETRm), the maximum light capture efficiency (α) and the maximum quantum yield (*Fv/Fm*) of PSII of *Sargassum fusiforme* and *Ulva lactuca* under different treatment conditions. Different lowercase letters represent significant differences. Long brackets indicate the statistical difference of increasing CO_2 concentration, and short brackets indicate the statistical difference of co-cultivation. * Represent the significant difference (*: $p < 0.05$; **: $p < 0.01$). Values represent means ± SD ($n = 3$).

3.4. Mannitol and pigment contents of *S. fusiforme*

Under ambient CO_2 concentration, co-culture ways significantly lower the content of mannitol of *S. fusiforme* ($p < 0.01$) (Fig. 4b). The content of mannitol of *S. fusiforme* was significantly increased by elevated CO_2 concentration only in monoculture ($p < 0.01$) (Fig. 4b).

Fig. 5 showed that co-culture ways significantly increased the contents of Chl *a* and the FPKM values of fucoxanthin-chlorophyll proteins (FCPs) in *S. fusiforme* under ambient CO_2 concentration ($p < 0.05$) (Fig. 5a, d). Under ambient CO_2 concentration, the Chl *c* content of *S. fusiforme* in co-culture was higher than that in other treatment ($p < 0.05$) (Fig. 5b). The content of Car decreased significantly by elevated CO_2 concentration in monoculture ($p < 0.05$) (Fig. 5c). Under high CO_2 concentration, Chl *a* content of *S. fusiforme* grown at co-culture was significantly higher than that under the conditions of monoculture and ambient CO_2 concentration ($p < 0.05$) (Fig. 5a).

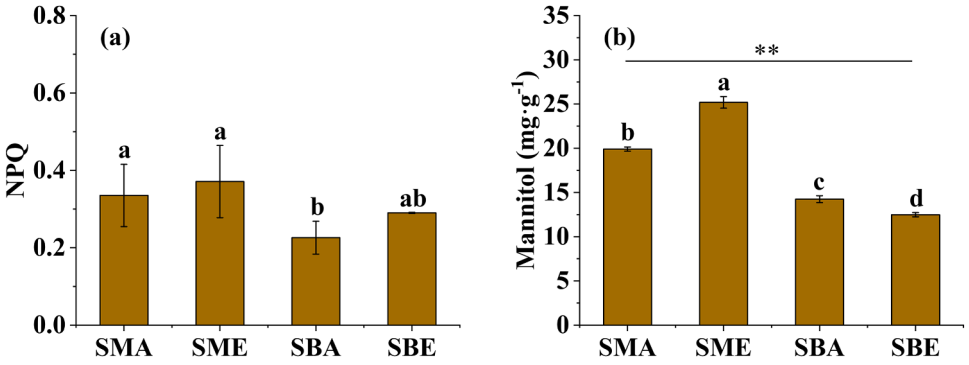

Fig. 4. The NPQ (a) and content of mannitol (b) of *Sargassum fusiforme* under different treatment conditions. Different lowercase letters represent significant differences. * Represent the significant difference between treatment groups (*: $p < 0.05$; **: $p < 0.01$). Values represent means ± SD ($n = 3$).

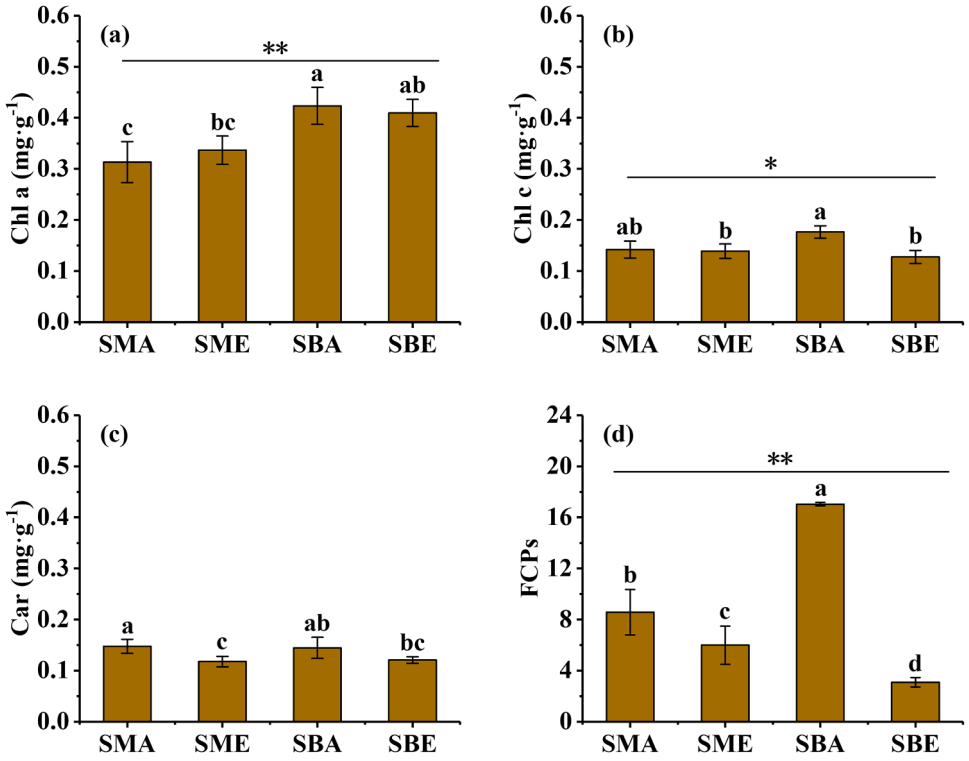

Fig. 5. The chlorophyll a (Chl *a*) (a), the chlorophyll c (Chl *c*) (b), the carotenoid (Car) (c) and the FPKM value of fucoxanthin-chlorophyll proteins (FCPs) (d) of *Sargassum fusiforme* under different treatment conditions. Different lowercase letters represent significant differences. * Represent the significant difference between treatment groups (*: $p < 0.05$; **: $p < 0.01$). Values represent means ± SD ($n = 3$).

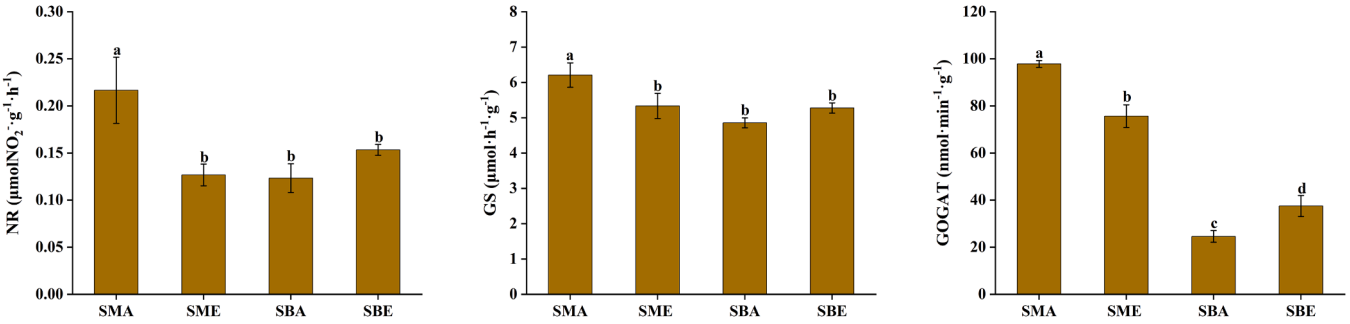

Fig. 6. The enzymes activities of nitrate reductase (NR) (a), glutamine synthetase (GS) (b) and glutamate synthase (GOGAT) (c) of *Sargassum fusiforme* under different treatment conditions. Different lowercase letters represent significant differences. Values represent means ± SD ($n = 3$).

3.5. Enzyme activity related to nitrogen metabolism

The activities of nitrate reductase (NR), glutamine synthetase (GS), and glutamate synthase (GOGAT) in *S. fusiforme* were significantly reduced under elevated CO_2 concentrations in monoculture conditions ($p < 0.05$) (Fig. 6a, b, c). Additionally, under ambient CO_2 conditions, the activities of these enzymes were also significantly lower in co-culture compared to monoculture ($p < 0.05$) (Fig. 6a, b, c). However, in co-culture, although high CO_2 concentrations increased NR and GS activities relative to ambient CO_2 conditions, these increases were not statistically significant ($p > 0.05$). In contrast, GOGAT activity was significantly higher under elevated CO_2 conditions in co-culture ($p < 0.05$) (Fig. 6a, b, c).

3.6. Comparative transcriptome analysis

The obtained transcriptome sequences were compared and annotated against the database (detailed data are provided in Supplementary Tables S3-S6 and Fig. S1-S2). As an initial step in analyzing the complex gene expression datasets, principal component analysis (PCA) was performed on the raw reads. Figure S3a illustrates significant differences in the cultivation of *S. fusiforme* compared to other cultivation methods under ambient CO_2 conditions and monoculture. Under monoculture conditions with elevated CO_2 concentration, *S. fusiforme* produced a total of 5209 unigenes, including 2687 up-regulated and 2522 down-regulated genes (Fig. S3b). Under ambient CO_2 conditions, co-cultivation with epibiotic *U. lactuca* resulted in 4779 unigenes, with 2500 up-regulated and 2279 down-regulated genes (Fig. S3c). Finally, under co-culture conditions with elevated CO_2, *S. fusiforme* eexpressed 4938 unigenes, of which 2549 were up-regulated and 2389 were down-regulated (Fig. S3d).

The Venn diagram (Fig. 7a) revealed that a total of 1905 genes exhibited differential expression patterns across different cultivation conditions. Specifically, comparisons were made between *S. fusiforme* cultivated under high CO_2 concentrations (SME) and the control group (SMA), *S. fusiforme* co-cultured with *U. lactuca* (SBA) and the control group (SMA), and the coupling conditions of high CO_2 concentration and co-culture with *U. lactuca* (SBE) compared to the control group (SMA). KEGG enrichment analysis was conducted on differentially expressed genes (DEGs) based on their enrichment levels and P-values. The top three significantly enriched pathways in the SME vs. SMA comparison were glutathione metabolism, ABC transporters, and

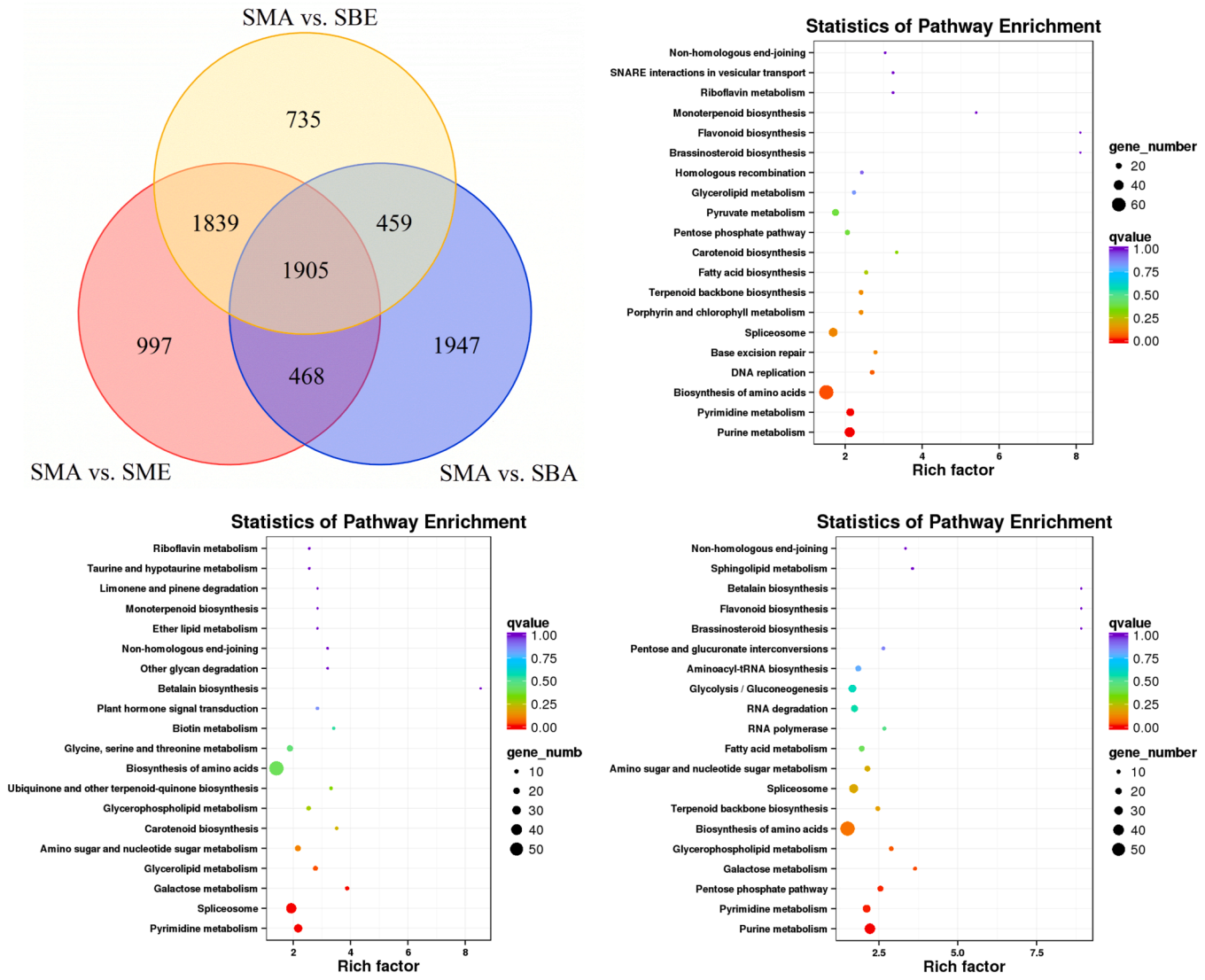

Fig. 7. Venn diagram of different expression genes (DEGs) (a), KEGG enrichment analysis of differential genes in *Sargassum fusiforme* grown under high CO_2 concentration (SMA vs. SME) (b), co-cultured with *Ulva lactuca* (SMA vs. SBA) (c), and the coupling conditions of high CO_2 concentration and co-culture (SMA vs. SBE) (d).

nitrogen metabolism (Fig. 7b). For the SBA vs. SMA comparison, the most significant pathway was associated with photosynthetic antenna proteins (Fig. 7c). In the SBE vs. SMA comparison, the significantly enriched pathways were primarily related to ABC transporters, pentose phosphate pathways, and nitrogen metabolism (Fig. 7d).

Thus, to further verify the effects of increased CO_2 concentration and interspecific competition of epiphytic *U. lactuca* on *S. fusiforme*, we anchored 10 metabolic pathways related to photosynthetic carbon assimilation and nitrogen metabolism, and initially screened DEGs in these pathways for analysis. A heat map was constructed to visualize the analysis results (Fig. 8).

3.7. Real-time quantitative polymerase chain reaction analysis

qRT-PCR analysis results of the six target genes are shown in Fig. 9. In *S. fusiforme* co-cultured with epiphytic *U. lactuca*, the expression of *GSH-Px* gene was significantly up-regulated ($p < 0.01$). Under high CO_2 concentration and co-culture with high CO_2 concentration conditions, the expression of the *GSH-Px* gene was up-regulated, although RNA-Seq showed no significant changes ($p > 0.05$). The gene expression levels of *LHC, RPE, GCL, GST*, and *6-PGDH* tended to be consistent in qRT-PCR and RNA-Seq analysis (Table S8).

3.8. Comparative transcriptomic analysis of SMA vs. SBA

It was observed from comparative transcriptome analysis that, the genes of photosystem I subunit (*PsaB*), photosystem II subunit (*PsbA, PsbC, PsbP, PsbO, PsbQ, PsbS*) and light harvesting complex (*LHCb4, LHCb5, LHCa4*) were extensively induced in *S. fusiforme* during co-culture with epiphytic *U. lactuca* ($p < 0.05$) (Fig. 8b). In addition, key genes involved in the Calvin cycle, such as the large subunits of ribulose-1,5-diphosphate carboxylase/oxygenase (Rubisco-LSMT) and phosphoglycerate kinase (PGK) were up-regulated, while glyceraldehyde-3-phosphate dehydrogenase (GAPDH) and triose-phosphateisomerase (TPI) were not significantly changed (Fig. 8a). These results indicated that genes related to photosynthetic carbon assimilation were differentially expressed at this stage. In the metabolic pathway of nitrogen assimilation, expression of key enzymes genes related to nitrogen assimilation, such as nitrite reductase (NiR), were down-regulated, except for glutamic dehydrogenase (GDH) ($p < 0.05$) (Fig. 8c). In addition, interspecific competition induced the expression of a wide range of enzyme genes involved in central metabolic pathways, including aconitase, isocitric dehydrogenase (IDH), and malate dehydrogenase (MDH) in the TCA cycle, as well as glutamate cysteine ligase (GCL), glutamyltransferase (GGT), glutathione-S-transferase (GST), and glutathione peroxidase (GPX) involved in the glutathione cycle ($p < 0.05$) (Fig. 8h, j).

3.9. Comparative transcriptomic analysis of SMA vs. SME

Compared with ambient CO_2 culture conditions, genes involved in photosynthetic carbon assimilation, such as glyceraldehyde-3-phosphate dehydrogenase (GAPDH), malate dehydrogenase (MDH), triose-phosphateisomerase (TPI), ribulose-1,5-diphosphate carboxylase/oxygenase (Rubisco), phosphoenolpyruvate carboxylase (PEPC) and phosphoglycerate kinase (PGK), were significantly upregulated under high CO_2 culture conditions. In contrast, NADP dependent malate enzyme (NADP-ME) and phosphoribulokinase (PRK) were significantly down-regulated ($p < 0.01$) (Fig. 8a). The expression and enzyme activity of Rubisco were increased under high CO_2 condition. In addition, gene expression of glucose-6-phosphate dehydrogenase (G6PDH) and phosphoglucomutase (PGLUM) involved in polysaccharide biosynthesis and mannitol-1-phosphate dehydrogenase (M1PDH) and mannitol-1-phosphatase (M1Pase) involved in mannitol metabolism pathway were up-regulated under elevated CO_2 ($p < 0.01$) (Fig. 8d, f, g).

Glycolysis-related genes such as enolase, pyruvate dehydrogenase complex (PDH E1, PDH E2), PGK, precursor of phosphoglycerate mutase (per-PGM), and glucose-6-phosphate isomerase (G6P1E), were up-

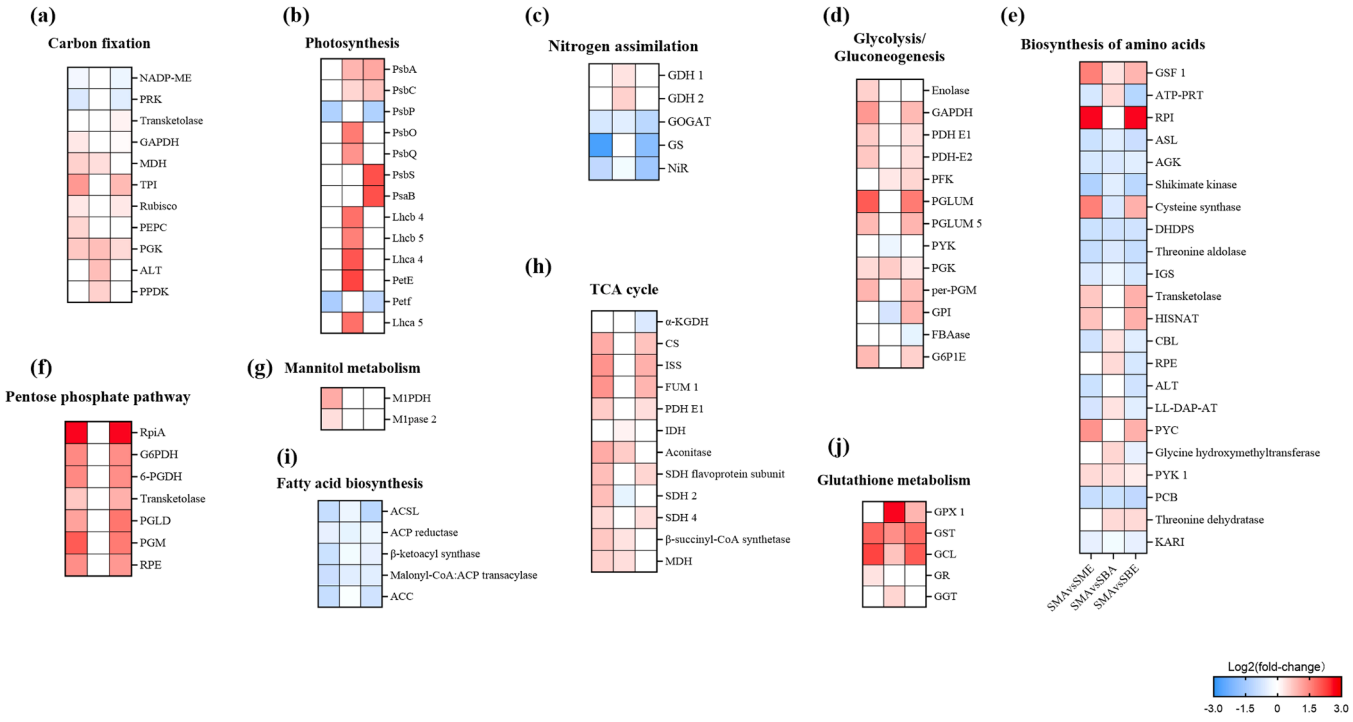

Fig. 8. Heatmap of the Expression change of DEGs involved in different culture groups; Rows represent genes with their name. The grouping from left to right indicate $\log_2$(fold-change) of genes at SMA vs. SME, SMA vs. SBA, SMA vs. SBE, respectively.
Note: Red spots represent up-regulated genes and blue spots indicate down-regulated genes. white spots represent genes that did not show significant changes between the control and treatment groups.

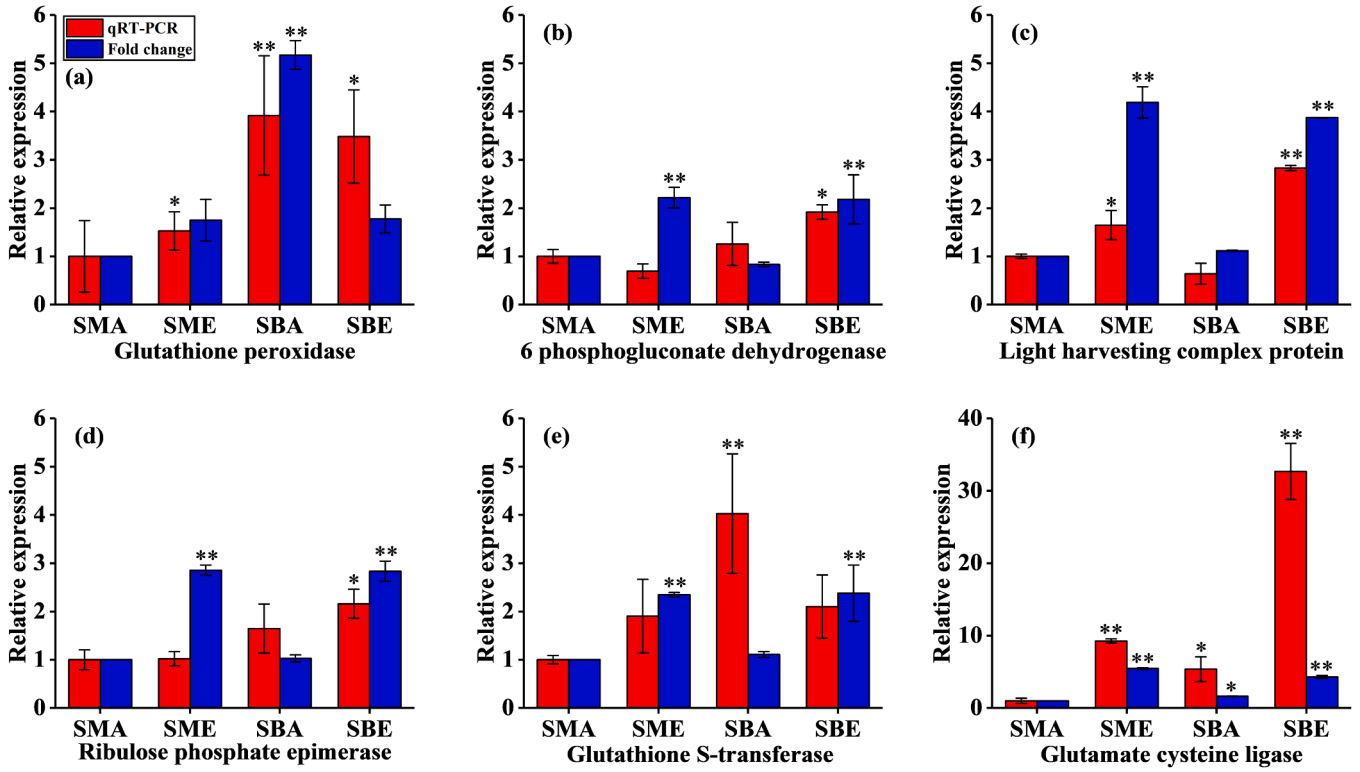

Fig. 9. Transcriptomic expression levels of six genes in different treatment groups. The differences of each gene are compared with the conditions of SMA. *: $P < 0.05$; **: $p < 0.01$.

regulated by elevated CO_2 ($p < 0.01$) (Fig. 8d), suggesting an enhanced glycolytic pathway. Genes involved in the TCA cycle including citrate synthase (CS), acetyl-CoA carboxylase (ISS), fumarate hydratase (FUM1), acontiase hydratase, succinate dehydrogenase subunits (SDH2, SDH4), malate dehydrogenase (MDH) and β-succinyl-CoA synthetase, were significantly upregulated under elevated CO_2 ($p < 0.01$) Fig. 8h). Under high CO_2 culture conditions, key genes involved in nitrogen assimilation pathway (NR, NiR, GOGAT) were down-regulated, indicating inhibited nitrogen assimilation ($p < 0.01$) (Fig. 8c). While genes associated with glutathione metabolism pathway (GST, GCL) were upregulated in the presence of elevated CO_2 ($p < 0.05$) (Fig. 8j).

3.10. Comparative transcriptomic analysis of SMA vs. SBE

Under the condition of elevated CO_2 concentration coupled with the epiphytic *U. lactuca*, the gene expression of photosystem I subunit (*PsaB*) and photosystem II subunits (*PsbA, PsbC, PsbS*) was upregulated ($p < 0.01$), indicating that the light-harvesting ability was activated and promoted electron transfer. Interestingly, we observed down-regulated expression of *PsbP* and ferredoxin genes (*PetF*), as shown in Fig. 8b ($p < 0.01$).

Similar to the conditions of increased CO_2 concentration, the key genes involved in carbon assimilation (Rubisco, transketoase, GAPDH, TPI, PGK) and the key genes involved in polysaccharide biosynthesis (G6PDH, phosphogluconolactonase (PGLD), phosphoglycerate mutase (PGM), RPE, glucose phosphate isomerase (GPI), PGLUM) were up-regulated ($p < 0.01$) (Fig. 8a, f). Moreover, coupling conditions also led to upregulations of glycolysis-related genes (PDH, phosphofructokinase (PFK), phosphoglycerate kinase (PGK), PGM, GPI) and TCA cycling-related genes (CS, ISS, FUM1, PDH E1, SDH4), which provided energy and intermediate metabolites in response to the effects of interspecific competition ($p < 0.01$) (Fig. 8d, h). Genes involved in nitrogen assimilation (NiR, GS, GOGAT) were further down-regulated, suggesting that coupling conditions had similar effects in inhibiting nitrogen assimilation as high CO_2 culture conditions ($p < 0.01$) (Fig. 8c).

4. Discussion

4.1. Effects of interspecific competition on S. fusiforme

U. lactuca is an epiphytic and competing genus of many economic seaweeds used in offshore cultivation (Björk et al., 2004; Chen et al., 2015; Liu et al., 2018, 2019a). In direct competitive interaction, resource competition is generally regarded as the main competitive mechanism affecting plant growth and photosynthesis. In this study, co-culture with *U. lactuca* significantly inhibited the rETRm, NPQ and growth of *S. fusiforme* at ambient CO_2 concentration. The thallu of *U. lactuca* are dark green in color and were consisted of lamellar leaves with dish-shaped fixators. The leaves of *U. lactuca* are long and wide, which can provide shade when attached to economic seaweed, reducing the photosynthetic electron transfer rate of seaweeds, including *S. fusiforme* (Baer and Stengel, 2014; Chen et al., 2015; Cao et al., 2022), thereby inhibiting the growth and photosynthesis of economic seaweeds. Sun (2021) found that when cultured with *U. prolifera, P. yezoensis*' growth rate was significantly inhibited along with a sharp decrease in photosynthetic activity. In addition, *Ulva* species such as *U. lactuca* have higher absorption rates of C and N nutrients, which is conducive to maintaining their interspecific competitive advantage with surrounding algae (Chen and Zou, 2015; Chen et al., 2017).

In this study, when co-cultured with *U. lactuca, PsbQ* and *PsbO* genes regulating photosynthetic oxygen-releasing complex (Liu et al., 2007) and *PetE*, an important gene for the synthesis plastocyanin-like protein (Pesaresi et al., 2009), were up-regulated in *S. fusiforme*. This suggested that PSI-related genes increased in response to competitive stress by *U. lactuca* in *S. fusiforme*. Under other interspecific stresses, such as microalgae, the expressions of PSI-related genes such as *PsaD, PsaE*, and *PsaG* in *S. fusiforme* were also up-regulated (Lin et al., 2021).

S. fusiforme also up-regulated expressions of light capture protein-

related genes under *U. lactuca* stress, while the rETRm of *S. fusiforme* was significantly decreased. Under co-culture conditions, the shading effects of *U. lactuca* prevented *S. fusiforme* from obtaining sufficient light energy to maintain its own photosynthesis (Naldi and Wheeler, 2002; Xu et al., 2010; Luo et al., 2012). When this occurred at ambient CO_2 concentration, *S. fusiforme* triggered the upregulation of a multitude of genes associated with photosynthesis to compensate for the shading by increasing its light harvesting antennae, including both PSII and PSI. This was consistent with the determination of Chl *a* content and the FPKM of FCPs.

In addition, *U. lactuca* absorbed a large amount of DIC benefit from its CO_2 concentration mechanisms (CCM) (Scoma et al., 2016). This stimulated the up-regulations of carbon assimilation related genes expressions in *S. fusiforme*. However, the expression of genes related to somatic cell elongation and maturation regulation in *S. fusiforme* was down-regulated (Table S7), and the increased dark respiration consumed a large amount of organic substances, resulting in a decrease in the mannitol content. This suggests that *S. fusiforme* is resistant to *U. lactuca* stress by up-regulating its carbon assimilation-related genes. In addition, this is an energy consuming process, as the Inorganic carbon transport into ribulose-1,5-bisphosphate carboxylase/oxygenase (RuBisCO) is one of the main limiting steps in carbon fixation, and upregulation of RuBisCo gene expression indicates an enhanced pathway for photosynthetic carbon fixation capacity, requiring the consumption of more ATP and NADPH (Singh et al., 2016). However, these energies and reducing forces are also required for nitrogen assimilation. Algae absorb NO_3^- from the environment, consume NADPH through nitrogen assimilation for reduction to produce NH_4^+, and then consume ATP through the glutamine synthetase/glutamate synthase pathway (GS/GOGAT) to promote the production of glutamine from NH_4^+ and glutamate, entering amino acid metabolism (De la Torre and Concepción., 2021). In this study, the activity of nitrogen assimilation related enzymes and gene expressions of *S. fusiforme* were significantly inhibited under co culture conditions, indicating that in interspecific competition, the presence of the competitive advantage species *U. lactuca* enhanced the carbon fixation pathway of *S. fusiforme* and inhibited its nitrogen assimilation ability, thereby affecting the balance of carbon and nitrogen allocation in the algal body.

4.2. Effect of elevated CO_2 concentration on S. fusiforme

In this study, elevated CO_2 concentration increased the DIC in seawater and promoted the growth of *S. fusiforme*. High CO_2 concentration caused seawater acidification, it was generally considered to positively affect the growth of *S. fusiforme* (Zou, 2005; Jiang et al., 2019; Wen and Zou, 2021). The photosynthesis rate of *S. fusiforme* increased significantly, as also expressed in increased rETRm, as the CO_2 concentrations increased. This indicated that ocean acidification was beneficial to the photosynthesis of *S. fusiforme*. At high CO_2 level, Pm enhancement of *S. fusiforme* may be demonstrated by down-regulation of flavodiiron proteins (FLV) or its homologous system, which can increase oxygen release, as performed in cyanobacteria and the green algae *Chlamydomonas* (Alboresi et al., 2019; Shimakawa et al., 2019). However, further research is needed to determine if the FLV or its homologous system is present in *S. fusiforme*.

Algae can regulate the expression of bicarbonate transporter, carbonic anhydrase, and genes related to the Calvin cycle under high CO_2 concentration (Hong et al., 2017; Hennon et al., 2019; Thangaraj and Sun., 2021). In this study, high CO_2 concentration had a great effect on *S. fusiforme. PsbP* encodes the oxygen-releasing complex peripheral protein in the PSII. Peripheral proteins are important for maintaining the functional integrity of the photosynthetic oxygen evolution complex (OEC) (Gnanasekaran et al., 2019). Interestingly, in the present research, the expression of *PsbP* in *S. fusiforme* was down-regulated with increasing the CO_2 concentration. However, the photosynthesis and growth of *S. fusiforme* were not significantly inhibited, indicating that down-regulated of *PsbP* had no obvious effects on the growth of *S. fusiforme*. Elevated CO_2 concentration also down-regulated the ferredoxin (Fd) gene (*PetF*) expression of *S. fusiforme*. Fd is an electron transfer protein in chloroplasts, which can release reducing equivalent from PSI of photosynthetic organisms (Arnon, 1988). Ferredoxin can also provide electrons for nitrite reductase (NiR), sulfite reductase (SiR) and fatty acid desaturase (FADs) for nitrogen and sulfur assimilation and fatty acid desaturation (Mulo., 2011; Walters and Golbeck., 2018). In this study, under the condition of elevated CO_2 concentration, the down-regulation of *PetF* had no effect on photosynthesis in *S. fusiforme*, but down-regulated the enzyme activities of NR, GOGAT and GS in the nitrogen assimilation pathway, as well as the expression levels of related genes, which may lead to inability of *S. fusiforme* to effectively utilize nitrate and nitrite in the environment. The gene expression of *LHCb5* and *LHCa3* antenna proteins in PSII of *S. fusiforme* were up-regulated with the increase in CO_2 concentrations, and the synthesis of the LHC in the photosystem of *S. fusiforme* was increased, resulting in promoted absorption in light energy.

Carbon assimilation is the process of reducing CO_2 to sugars through the assimilative powers of light reactions (ATP and NADPH) (Johnson, 2016). This process takes place in chloroplast stroma and involves many enzymes such as *GAPDH, RPE*, and *RPI*. In this study, gene expression of these enzymes increased with increasing CO_2 concentrations. Meanwhile, the genes of key enzymes M1PDH and M1Pase in the mannitol pathway, as well as Phosphoglucomutase (PGLUM) in the glycogen synthesis pathway also showed an up-regulation trend. The results showed that the increase of CO_2 in seawater had fertilization effect on *S. fusiforme*. This improved the photosynthetic carbon assimilation efficiency and promoted the growth of *S. fusiforme*. As the CO_2 concentrations were elevated, the concentration of HCO_3^- increased and *S. fusiforme* transformed more HCO_3^- into CO_2 (using extracellular carbonic anhydrase), which diffused into algal cells (Zou et al., 2003). The increase in CO_2 concentration in the cells increased the enzyme genes expressions for carbon assimilation, meaning improved photosynthetic carbon assimilation efficiency. This provided sufficient carbon skeleton and organic matter for mannitol accumulation and the growth of *S. fusiforme*. In this study, high CO_2 concentration increased the carbon assimilation of *S. fusiforme* (Fig. 10). Similar results have been found in studies involving other algae (Wu et al., 2010; Wei et al., 2021).

4.3. Effects of interspecific competition on S. fusiforme under elevated CO_2 concentrations

Ulva species have strong photosynthesis and ability to absorb of C and N nutrients (Chen and Zou, 2015; Chen et al., 2017). Co-culture with *U. lactuca* inhibited the growth and photosynthesis of *S. fusiforme*, but the growth, rETRm, *Fv/Fm* of *S. fusiforme* significantly increased with the increase of CO_2 concentration. Ocean acidification have been shown to mitigate the harmful effects of abiotic stresses (high temperature, drought, and salinity) in plants (Gill and Tuteja, 2010; AbdElgawad et al., 2015; Uddin et al., 2018). In this study, although the activities of nitrogen assimilation-related enzymes in *S. fusiforme* were inhibited to varying degrees under different treatments, it is noteworthy that elevated CO_2 concentration significantly promoted GOGAT activity in this algae compared to co-culture conditions. GOGAT utilizes electrons from NADPH produced during photosynthesis to convert glutamine and α-ketoglutarate (α-KG) into glutamate, thereby providing a foundation for amino acid metabolism and alleviating interspecific competition stress.

In this study, under the conditions of co-culture and elevated CO_2 concentration, the expression of *PsaB* and *PsbA* genes in *S. fusiforme* was up-regulated, indicating activation of light-harvesting capabilities that promote electron transport. It was found that the upregulation of *PsbA, PsbB, PsbC*, and *PsbD* genes would accelerate electron transfer, when studying the effect of copper on photosynthesis of *Dunaliella salina* (Ling et al., 2021). Under co-culture conditions, due to the competitive

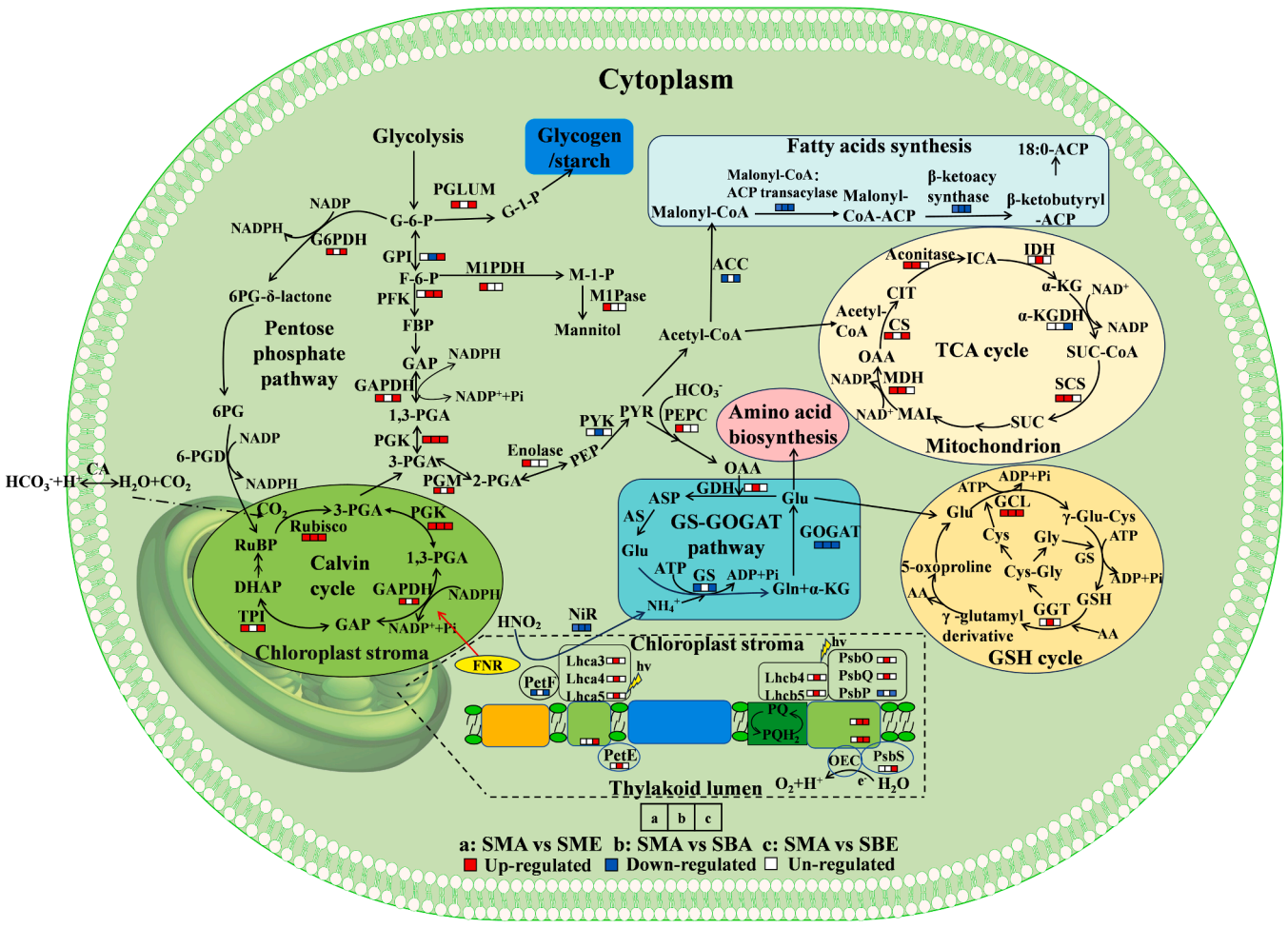

Fig. 10. Pattern diagram of change mechanism of photosynthetic carbon assimilation in *Sargassum fusiforme* under interspecific stress of epiphytic *Ulva lactuca* and elevated CO_2 concentration. The blue filled box, red filled box, and white filled box represent genes downregulated, upregulated, and undifferentiated, respectively. The a in the box represents the DEGs in *S. fusiforme* grown under high CO_2 concentration (SMA vs. SME). The b in the box represents the DEGs in *S. fusiforme* co-cultured with *U. lactuca* (SMA vs. SBA). The c in the box represents the DEGs in *S. fusiforme* grown under the coupling conditions of high CO_2 concentration and co-culture (SMA vs. SBE).

utilization of DIC by *U. lactuca*, in *S. fusiforme*, the electrons provided by PSI could not effectively used for carbon fixation or for non-existent alternative sinks. These extra electrons could cause oxidative damage as PSI produces superoxide and H_2O_2, which was dangerous to PSI, if PSII keeps on donating electrons (Lima-Melo et al., 2019; He et al., 2021). Thus, *S. fusiforme* down-regulated PSII (*PsbP*) to protect PSI and other components of the chloroplast from excessive ROS damage. However, *S. fusiforme* can still express *PsbA* at the transcriptional level. *PsbA* is the coding gene encoding D1 protein in PSII, and the expression of these chloroplast genes is mostly regulated at the translational level (Sun and Zerges, 2015). The up-regulated expression of *PsbA* can enhance performance of PSII repair system (Tyystjarvi and Aro, 1996; Nishiyama and Murata, 2014; Chotewutmontri and Barkan, 2020), but increase energy consumption. This resulted in inhibited photosynthesis and decreased mannitol contents, and finally decreased the growth of *S. fusiforme*.

When the CO_2 level was elevated, *S. fusiforme* had enough CO_2 for carbon assimilation. Due to decreased oxidative damage caused by extra electrons, the increase in CO_2 concentration alleviated the inhibition of *S. fusiforme* growth and photosynthesis from epiphytic *U. lactuca*. However, it was found that the growth of *G. lemaneiformis* was more evidently inhibited when the CO_2 concentration elevated (Chen et al., 2015). This is probably resulted from the different responses of seaweeds to elevated CO_2 concentration for their variant metabolic process (Yadav and Mishra, 2020). Under high CO_2 conditions, the culture medium provided adequate DIC. The up-regulated of genes involved in photosynthetic carbon assimilation produced a large amount of energy and organic matter that enabled the *S. fusiforme* to resist *U. lactuca* stress (Fig. 10). The excess energy can also be used for algal growth, as demonstrated by the significant increase in the relative growth rate of *S. fusiforme* under the treatment conditions.

In conclusion, when co-cultured with epiphytic *U. lactuca, S. fusiforme* exhibited increased expression of light-harvesting complex proteins and carbon assimilation genes, while nitrogen assimilation efficiency was reduced. Consequently, this altered the carbon and nitrogen metabolism, enabling *S. fusiforme* to resist epiphytic stress. Ocean acidification regulated the electron transport between PSI and PSII by increasing the expressions of antenna protein and carbon assimilation-related enzyme genes required for photosynthesis, thus promoting photosynthesis and growth of *S. fusiforme*. These results indicated that elevated CO_2 concentration alleviated epiphytic stress by regulating the photosynthetic system (PSI and PSII) and carbon nitrogen metabolism strategies. In terms of climate change, ocean acidification induced by increasing atmospheric CO_2 concentrations and interspecific competition are the two main factors affecting offshore macroalgae culture. This study is of great significance to further study the culture management of *S. fusiforme* under the background of climate change, and to explore the ecological significance and carbon sequestration efficiency of seaweed

farming in the future.

CRediT authorship contribution statement

Cong Cao: Writing – original draft, Visualization, Methodology, Investigation, Data curation, Conceptualization. **Dongya Bao:** Writing – original draft, Visualization, Investigation, Data curation. **Lili Xu:** Investigation, Data curation. **Zengling Ma:** Supervision, Resources, Project administration, Funding acquisition, Formal analysis. **Mingjiang Wu:** Supervision, Resources, Project administration, Funding acquisition. **Guang Gao:** Supervision, Methodology, Formal analysis. **Kit Wayne Chew:** Supervision, Methodology, Formal analysis. **Shuaipeng Tian:** Visualization, Investigation, Data curation. **Binbin Chen:** Writing – review & editing, Supervision, Resources, Project administration, Methodology, Funding acquisition, Formal analysis, Conceptualization.

Declaration of competing interest

The authors declare the following financial interests/personal relationships which may be considered as potential competing interests:

Mingjiang Wu reports financial support was provided by National Key Research and Development Program of China. Binbin Chen reports financial support was provided by Wenzhou Science and Technology Plan Project. Binbin Chen reports financial support was provided by Wenzhou Science and Technology Plan Project. No conflicts of interest declared. If there are other authors, they declare that they have no known competing financial interests or personal relationships that could have appeared to influence the work reported in this paper.

Acknowledgments

This work was supported by the Wenzhou Science and Technology Plan Project (No. ZX2024003-4 and N20220005), the National Key Research and Development Program of China (No. 2018YFD0901500), the National Natural Science Foundation of China (No. 41706147 and 41876124). The authors also would like to appreciate all staffs for their helpful assistance during the materials collection and for editing and proofreading the manuscript.

Supplementary materials

Supplementary material associated with this article can be found, in the online version, at doi:10.1016/j.hal.2025.102908.

Data availability

The processed data is available in the Supplementary tables provided.

References

AbdElgawad, H., Farfan-Vignolo, E.R., Vos, D.d., Asard, H., 2015. Elevated CO_2 mitigates drought and temperature-induced oxidative stress differently in grasses and legumes. Plant Sci. (Limerick) 231, 1–10. https://doi.org/10.1016/j.plantsci.2014.11.001.

Albert, G., Hepburn, C.D., Pajusalu, L., Paalme, T., Pritchard, D.W., Martin, G., 2020. Could ocean acidification influence epiphytism? A comparison of carbon-use strategies between *Fucus vesiculosus* and its epiphytes in the baltic sea. J. Appl. Phycol. 32 (4), 2479–2487. https://doi.org/10.1007/s10811-019-01953-z.

Alboresi, A., Storti, M., Morosinotto, T., 2019. Balancing protection and efficiency in the regulation of photosynthetic electron transport across plant evolution. New. Phytol. 221, 105–109. https://doi.org/10.1111/nph.15372.

Arnon, D.I., 1988. The discovery of ferredoxin: the photosynthetic path. Trends. Biochem. Sci. 13, 30–33. https://doi.org/10.1016/0968-0004(88)90016-3.

Axelsson, L., Larsson, C., Ryberg, H., 1999. Affinity, capacity and oxygen sensitivity of two different mechanisms for bicarbonate utilization in *Ulva lactuca* L. (chlorophyta). Plant, Cell Environ. 22, 969–978. https://doi.org/10.1046/j.1365-3040.1999.00470.x.

Ayache, N., Lundholm, N., Gai, F., Hervé, F., Amzil, Z., Caruana, A., 2021. Impacts of ocean acidification on growth and toxin content of the marine diatoms *Pseudo-nitzschia australis* and *P. fraudulenta*. Mar. Environ. Res. 169, 105380. https://doi.org/10.1016/j.marenvres.2021.105380.

Baer, J., Stengel, D.B., 2014. Can native epiphytes affect establishment success of the alien seaweed *Sargassum muticum* (Phaeophyceae)? Biol. Environ.: Proc. R. Irish Acad. 114, 41–52. https://doi.org/10.3318/BIOE.2014.05.

Barakat, K.M., El-Sayed, H.S., Khairy, H.M., El-Sheikh, M.A., 2021. Effects of ocean acidification on the growth and biochemical composition of a green alga (*Ulva fasciata*) and its associated microbiota. Saudi. J. Biol. Sci. 28, 5106–5114. https://doi.org/10.1016/j.sjbs.2021.05.029.

Behrenfeld, M.J., Marañón, E., Siegel, D.A., Hooker, S.B., 2002. Photoacclimation and nutrient-based model oflight-saturated photosynthesis for quantifying oceanic primary production. Mar. Ecol. Prog. Ser. 228, 103–117. https://doi.org/10.3354/meps228103.

Benjamini, Y., Hochberg, Y., 1995. Controlling the false discovery rate a practical and powerful approach to multiple testing. J. R. Stat. Soc. Ser. B, Stat. Methodol. 57, 289–300.

Björk, M., Axelsson, L., Beer, S., 2004. Why is *Ulva* intestinalis the only macroalga inhabiting isolated rockpools along the Swedish Atlantic coast? Mar. Ecol. Prog. Ser. 283, 109–116.

Cao, C., Zhang, T., Wu, M., Chen, B., Ma, Z., 2022. Differential growth and physiological responses of *Sargassum fusiforme* and epiphytic *ulva lactuca* to culture densities and interspecific competition. Reg. Stud. Mar. Sci. 56, 102671. https://doi.org/10.1016/j.rsma.2022.102671.

Chen, B., Gu, Z., Wu, M., Ma, Z., Lim, H.R., Khoo, K.S., Show, P.L., 2022. Advancement pathway of biochar resources from macroalgae biomass: a review. Biomass Bioenergy 167, 106650. https://doi.org/10.1016/j.biombioe.2022.106650.

Chen, B., Lin, L., Ma, Z., Zhang, T., Chen, W., Zou, D., 2019a. Carbon and nitrogen accumulation and interspecific competition in two algae species, *Pyropia haitanensis* and *Ulva lactuca*, under ocean acidification conditions. Aquacult. Int. 27, 721–733. https://doi.org/10.1007/s10499-019-00360-y.

Chen, B., Zou, D., 2015. Altered seawater salinity levels affected growth and photosynthesis of *ulva fasciata* (Ulvales, Chlorophyta) germlings. Acta Oceanol. Sin. 8, 108–113. https://doi.org/10.1007/s13131-015-0654-3.

Chen, B., Zou, D., Jiang, H., 2015. Elevated CO.sub.2 exacerbates competition for growth and photosynthesis between *Gracilaria lemaneiformis* and *Ulva lactuca*. Aquaculture 443, 49–55. https://doi.org/10.1016/j.aquaculture.2015.03.009.

Chen, B., Zou, D., Zhu, M., 2017. Growth and photosynthetic responses of *Ulva lactuca* (Ulvales, Chlorophyta) germlings to different pH levels. Mar. Biol. Res. 13, 351–357. https://doi.org/10.1080/17451000.2016.1267367.

Chen, B., Zou, D., Ma, Z., Yu, P., Wu, M., 2019b. Effects of light intensity on the photosynthetic responses of *Sargassum fusiforme* seedlings to future CO_2 rising. Aquacult. Res. 50, 116–125. https://doi.org/10.1111/are.13873.

Chen, X., Nie, W., Yu, G., Li, Y., Hu, Y., Lu, J., Jin, L., 2012. Antitumor and immunomodulatory activity of polysaccharides from *Sargassum fusiforme*. Food Chem. Toxicol. 50, 695–700. https://doi.org/10.1016/j.fct.2011.11.015.

Chotewutmontri, P., Barkan, A., 2020. Light-induced PsbA translation in plants is triggered by photosystem II damage via an assembly-linked autoregulatory circuit. Proc. Natl. Acad. Sci. – PNAS. 117, 21775–21784. https://doi.org/10.1073/pnas.2007833117.

Chukhutsina, V.U., Liu, X., Xu, P., Croce, R., 2020. Light-harvesting complex II is an antenna of photosystem I in dark-adapted plants. Nat. Plants. 6 (7), 860. https://doi.org/10.1038/s41477-020-0693-4.

Corzo, A., Niell, F.X., 1991. Determination of nitrate reductase activity in *ulva* rigida C. Agardh by the in-situ method. J. Exp. Mar. Biol. Ecol. 146, 181–191. https://doi.org/10.1016/0022-0981(91)90024-Q.

De Ramos, B., Da Costa, G.B., Ramlov, F., Maraschin, M., Horta, P.A., Figueroa, F.L., Korbee, N., Bonomi-Barufi, J., 2019. Ecophysiological implications of UV radiation in the interspecific interaction of *Pyropia acanthophora* and *Grateloupia turuturu* (Rhodophyta). Mar. Environ. Res. 144, 36–45. https://doi.org/10.1016/j.marenvres.2018.11.014.

De la Torre, F., Avila, C., 2021. Special issue editorial: plant nitrogen assimilation and metabolism. Plants-Basel. 10, 2223–7747. https://doi.org/10.3390/plants10071278.

Doney, S.C., Fabry, V.J., Feely, R.A., Kleypa, s J.A., 2009. Ocean acidification: the other CO_2 problem. Ann. Rev. Mar. Sci. 1, 169–192. https://doi.org/10.1146/annurev.marine.010908.163834.

Dominguez, H., Loret, E.P., 2019. *Ulva lactuca*, A source of troubles and potential riches. Mar. Drugs 17, 357–377. https://doi.org/10.3390/md17060357.

Friedlander, M., 1992. *Gracilaria conferta* and its epiphytes the effect of culture conditions on growth. Bot. Mar. 35, 423–428. https://doi.org/10.1515/botm.1992.35.5.423.

Froehlich, H.E., Afflerbach, J.C., Frazier, M., Halpern, B.S., 2019. Blue growth potential to mitigate climate change through seaweed offsetting. Curr. Biol. 29. https://doi.org/10.1016/j.cub.2019.07.041, 3087-3093.e3.

Gattuso, J., Magnan, A., Bille, R., Cheung, W.W.L., Howes, E.L., Jood, F., Allemand, D., Bopp, L., Cooley, S.R., Eakin, C.M., Hoegh-Guldberg, O., Kelly, R.P., Poritner, H.O., Drogers, A.D., Baxter, J.M., Laffoley, D., Osborn, D., Rankovic, A., Rochette, J., Sumaila, U.R., Treyer, S., Turley, C., 2015. Contrasting futures for ocean and society from different anthropogenic CO_2 emissions scenarios. Science (1979) 349 (6243). https://doi.org/10.1126/science.aac4722.

Gao, G., Fu, Q., Beardall, J., Wu, M., Xu, J., 2019. Combination of ocean acidification and warming enhances the competitive advantage of *Skeletonema costatum* over a green tide alga, *Ulva linza*. Harmful. Algae 85, 101698. https://doi.org/10.1016/j.hal.2019.101698.

Gao, K., Aruga, J.M., Coronil, T., 1993. Influence of enhanced CO_2 on growth and photosynthesis of the red algae *gracilaria* sp. and *G. chilensis*. J. Appl. Phycol. 5 (6), 563–571. https://doi.org/10.1007/BF02184635.

Garcia-Redondo, V., Barbara, I., Diaz-Tapia, P., 2019. Biodiversity of epiphytic macroalgae (Chlorophyta, Ochrophyta, and Rhodophyta) on leaves of *Zostera marina* in the northwestern Iberian Peninsula. Anal. Jardín Bot. Madrid (1979). 76, 78–e078. https://doi.org/10.3989/ajbm.2502.

Genty, B., Briantais, J., Baker, N.R., 1989. The relationship between the quantum yield of photosynthetic electron transport and quenching of chlorophyll fluorescence. Biochim. Biophys. Acta Gen. Subj. 990, 87–92. https://doi.org/10.1016/S0304-4165(89)80016-9.

Gill, S.S., Tuteja, N., 2010. Reactive oxygen species and antioxidant machinery in abiotic stress tolerance in crop plants. Plant Physiol. Biochem. 48, 909–930. https://doi.org/10.1016/j.plaphy.2010.08.016.

Gnanasekaran, P., Ponnusamy, K., Chakraborty, S., 2019. A geminivirus betasatellite encoded βC1 protein interacts with PsbP and subverts PsbP-mediated antiviral defence in plants. Mol. Plant Pathol. 20, 943–960. https://doi.org/10.1111/mpp.12804.

Gran, G., 1952. Determination of the equivalence point in potentiometric titrations of sea water with hydrochloric acid. Oceanol. Acta. 209–218.

Hartmann, J., West, A.J., Renforth, P., et al., 2013. Enhanced chemical weathering as a geoengineering strategy to reduce atmospheric carbon dioxide, supply nutrients, and mitigate ocean acidification. Rev. Geophys. 51 (1985), 113–149. https://doi.org/10.1002/rog.20004.

He, W., Yan, K., Zhang, Y., et al., 2021. Contrasting photosynthesis, photoinhibition and oxidative damage in honeysuckle (*Lonicera japonica* Thunb.) under iso-osmotic salt and drought stresses. Environ. Exp. Bot. 182. https://doi.org/10.1016/j.envexpbot.2020.104313.

He, Y., Ma, Y., Du, Y., Shen, S., 2018. Differential gene expression for carotenoid biosynthesis in a green alga *ulva prolifera* based on transcriptome analysis. BMC. Genomics. 19 (1), 916. https://doi.org/10.1186/s12864-018-5337-y.

Hennon, G.M.M., Williamson, O.M., Hernández Limón, M.D., Haley, S.T., Dyhrman, S.T., 2019. Non-linear physiology and gene expression responses of harmful alga *heterosigma akashiwo* to rising CO_2. Protist. 170 (1), 38–51. https://doi.org/10.1016/j.protis.2018.10.002.

Hill, R., Bellgrove, A., Macreadie, P.I., Petrou, K., Beardall, J., Steven, A., Ralph, P.J., 2015. Can macroalgae contribute to blue carbon? An Australian perspective. Limnol. Oceanogr. 60, 1689–1706. https://doi.org/10.1002/lno.10128.

Hong, H., Shen, R., Zhang, F., Wen, Z., Chang, S., Lin, W., Kranz, S.A., Luo, Y.-W, Kao, S.-J., Morel, F.M.M., Shi, D., 2017. The complex effects of ocean acidification on the prominent N_2-fixing cyanobacterium *trichodesmium*. Science (1979) 356 (6337), 527–531. https://doi.org/10.1126/science.aal2981.

Ji, Z., Zou, D., Gong, J., Liu, C., Ye, C., Chen, Y., 2019. The different responses of growth and photosynthesis to NH_4^+ enrichments between *Gracilariopsis lemaneiformis* and its epiphytic alga *ulva lactuca* grown at elevated atmospheric CO_2. Mar. Pollut. Bull. 144, 173–180. https://doi.org/10.1016/j.marpolbul.2019.04.049.

Jia, R., Li, Z., Wu, J., Ou, Z., Zhu, Q., Sun, B., Lin, L., Zhao, M., 2020. Physicochemical properties of polysaccharide fractions from *Sargassum fusiforme* and their hypoglycemic and hypolipidemic activities in type 2 diabetic rats. Int. J. Biol. Macromol. 147, 428–438. https://doi.org/10.1016/j.ijbiomac.2019.12.243.

Jiang, H., Zou, D., Lou, W., Gong, J., 2019. Effects of CO_2 supply on growth and photosynthetic ability of young sporophytes of the economic seaweed *Sargassum fusiforme* (Sargassaceae, Phaeophyta). J. Appl. Phycol. 31, 615–624. https://doi.org/10.1007/s10811-018-1569-0.

Johnson, M.P., 2016. photosynthesis. Essays Biochem. 60, 255–273. https://doi.org/10.1042/EBC20160016.

Kang, E.J., Kim, K.Y., 2016. Effects of future climate conditions on photosynthesis and biochemical component of *Ulva pertusa* (Chlorophyta). Algae 31, 49–59. https://doi.org/10.4490/algae.2016.31.3.9.

Kang, J.W., Chung, I.K., 2017. The effects of eutrophication and acidification on the ecophysiology of *Ulva pertusa* Kjellman. J. Appl. Phycol. 29, 2675–2683. https://doi.org/10.1007/s10811-017-1087-5.

Kerrison, P., Suggett, D.J., Hepburn, L.J., Steinke, M., 2012. Effect of elevated pCO_2 on the production of dimethylsulphoniopropionate (DMSP) and dimethylsulphide (DMS) in two species of *Ulva* (Chlorophyceae). Biogeochemistry. 110, 5–16. https://doi.org/10.1007/s10533-012-9707-2.

Key, R.M., Yamanaka, Y., Joos, F., et al., 2005. Anthropogenic ocean acidification over the twenty-first century and its impact on calcifying organisms. Nature 437, 681–686. https://doi.org/10.1038/nature04095.

Kokubu, S., Nishihara, G.N., Watanabe, Y., Tsuchiya, Y., Amamo, Y., Terada, R., 2015. The effect of irradiance and temperature on the photosynthesis of a native alga *sargassum fusiforme* (Fucales) from Kagoshima, Japan. Phycologia (Oxford) 54, 235–247. https://doi.org/10.2216/15-007.1.

Krause-Jensen, D., Duarte, C., 2016. Substantial role of macroalgae in marine carbon sequestration. Nat. Geosci. 9, 737–742. https://doi.org/10.1038/ngeo2790.

Lewis, E., Wallace, D.W.R., 1998. Program developed for CO_2system calculations. ORNL/CDIAC-105. Carbon Dioxide Information Analysis Center. Oak Ridge National Laboratory, US Department of Energy, Oak Ridge, Tennessee.

Liang, W., Ouyang, S., Shaw, N., Joachimiak, A., Zhang, R., Liu, Z., 2011. Conversion of D-ribulose 5-phosphate to D-xylulose 5-phosphate: new insights from structural and biochemical studies on human RPE. FASEB J. 25 (2), 497. https://doi.org/10.1096/fj.10-171207.

Lima-Melo, Y., Alencar, Vicente, et al., 2019. Photoinhibition of photosystem I provides oxidative protection during imbalanced photosynthetic electron transport in Arabidopsis thaliana. Front. Plant Sci. 10, 916–929. https://doi.org/10.3389/fpls.2019.00916.

Lin, L., Chen, B., Wang, S., Li, J., Ma, Z., 2021. Comparative transcriptome and cross-section analyses provide insights into the mechanisms underlying *Sargassum fusiforme* responses to the harmful algal bloom-forming dinoflagellate *Karenia mikimotoi*. Aquat. Bot. 172, 103383. https://doi.org/10.1016/j.aquabot.2021.103383.

Lin, G., Yao, J., Yang, J., 2014. Research on extraction technology of polysaccharides and mannitols from Laminaria Japonica. J. Fujian Fisheries 36, 205–210 (In Chinese with English abstract).

Lin, L., Shang, T., Zhang, T., Wang, C., Chen, B., Wu, M., Ma, Z., 2020. Supplementary study on reproductive biology and life cycle of *Sargassum fusiforme* (Phaeophyceae). J. Fisheries China. 44, 581–595 (In Chinese with English abstract).

Ling, N., Li, W., Xu, G., Qi, Z., Ji, C., Liu, X., Cui, D., Sun, Y., 2021. Transcriptomic sequencing reveals the response of *Dunaliella salina* to copper stress via the increased photosynthesis and carbon metabolisms. Mol. Omics. 17, 769–782. https://doi.org/10.1039/D1MO00125F.

Liu, C., Zou, D., Yang, Y., 2018. Comparative physiological behaviors of *ulva lactuca* and *gracilariopsis lemaneiformis* in responses to elevated atmospheric CO_2 and temperature. Environ. Sci. Pollut. Res. Int. 25, 27493–27502. https://doi.org/10.1007/s11356-018-2792-6.

Liu, H., Frankel, L.K., Bricker, T.M., 2007. Functional analysis of photosystem II in a psbO-1-deficient mutant in *Arabidopsis thaliana*. Biochemistry (Easton) 46, 7607–7613. https://doi.org/10.1021/bi700107w.

Liu, J., Wu, S., Chen, L., et al., 2020. Different extraction methods bring about distinct physicochemical properties and antioxidant activities of *Sargassum fusiforme* fucoidans. Int. J. Biol. Macromol. 155, 1385–1392. https://doi.org/10.1016/j.ijbiomac.2019.11.113.

Liu, Y., Cao, J., Chu, Y., Liu, Y., Wang, Q., Gong, Q., Li, J., 2021. The brown algae *Saccharina japonica* and *sargassum horneri* exhibit species-specific responses to synergistic stress of ocean acidification and eutrophication. J. Ocean. Univ. China 20, 1253–1262. https://doi.org/10.1007/s11802-021-4853-6.

Luo, L., Zuo, X., Chen, B., 2023. Effects of exogenous hormones on the regeneration of juveniles from *Sargassum fusiforme* holdfasts. Front. Mar. Sci. 9. https://doi.org/10.3389/fmars.2022.1072391.

Luo, M.B., Liu, F., Xu, Z.L., 2012. Growth and nutrient uptake capacity of two co-occurring species, *Ulva prolifera* and *Ulva linza*. Aquat. Bot. 100, 18–24. https://doi.org/10.1016/j.aquabot.2012.03.006.

Livak, K.J., Schmittgen, T.D., 2001. Analysis of relative gene expression data using real-time quantitative PCR and the 2(-Delta Delta C(T)) method. Methods 25 (4), 402–408. https://doi.org/10.1006/meth.2001.1262.

Mortazavi, A., Williams, B.A., McCue, K., Schaeffer, L., Wold, B., 2008. Mapping and quantifying mammalian transcriptomes by RNA-seq. Nat. Methods 5 (7), 621–628. https://doi.org/10.1038/nmeth.1226.

Mulo, P., 2011. Chloroplast-targeted ferredoxin-NADP (+) oxidoreductase (FNR): structure, function and location. Biochim. Biophys. Acta 1807, 927–934. https://doi.org/10.1016/j.bbabio.2010.10.001.

Naldi, M., Wheeler, P., 2002. N-15 measurements of ammonium and nitrate uptake by *Ulva fenestrata* (Chlorophyta) and *Gracilaria pacifica* (Rhodophyta): comparison of net nutrient disappearance, release of ammonium and nitrate, and N-15 accumulation in algal tissue. J. Phycol. 38, 135–144. https://doi.org/10.1046/j.1529-8817.2002.01070.x.

Nishiyama, Y., Murata, N., 2014. Revised scheme for the mechanism of photoinhibition and its application to enhance the abiotic stress tolerance of the photosynthetic machinery. Appl. Microbiol. Biotechnol. 98, 8777–8796. https://doi.org/10.1007/s00253-014-6020-0.

Okada, M., Kimura, Y., 2022. Characterization of glutamate-cysteine ligase and glutathione synthetase from the δ-proteobacterium myxococcus xanthus. Proteins, Struct., Funct. Bioinformat. 90 (8), 1547–1560. https://doi.org/10.1002/prot.26333.

Panday, S., Talreja, R., Kavdia, M., 2020. The role of glutathione and glutathione peroxidase in regulating cellular level of reactive oxygen and nitrogen species. Microvasc. Res. 131, 104010.

Parsons, T.R., Strickland, J.D.H., 1963. Discussion of spectrophotometric determination of marine plant pigments, with revised equations for ascertaining chlorophylls and carotenoids. J. Mater. Res. 21, 155–163.

Peña, V., Harvey, B.P., Agostini, S., Porzio, L., Milazzo, M., Horta, P., 2021. Major loss of coralline algal diversity in response to ocean acidification. Glob. Chang. Biol. 27, 4785–4798. https://doi.org/10.1111/gcb.15757.

Pesaresi, P., Scharfenberg, M., Weigel, M., et al., 2009. Mutants, over expressors, and interactors of *Arabidopsis* plastocyanin isoforms: revised roles of plastocyanin in photosynthetic electron flow and thylakoid redox state. Mol. Plant 2, 236–248. https://doi.org/10.1093/mp/ssn041.

Platt, T., Gallegos, C.L., Harrison, W.G., 1980. Photoinhibition of photosynthesis in natural assemblages of marine phytoplankton. J. Mar. Res. 38, 687–701.

Porra, R.J., 2002. The chequered history of the development and use of simultaneous equations for the accurate determination of chlorophylls *a* and *b*. Photosynth. Res. 73, 149–156. https://doi.org/10.1023/A:1020470224740.

Raven, J.A., Hurd, C.L., 2012. Ecophysiology of photosynthesis in macroalgae. Photosyn. Res. 113, 105–125. https://doi.org/10.1007/s11120-012-9768-z.

Schulze, S.K., Kanwar, R., Gölzenleuchter, M., Therneau, T.M., Beutler, A.S., 2012. SERE: single-parameter quality control and sample comparison for RNA-seq. BMC. Genomics. 13, 1–9. https://doi.org/10.1186/1471-2164-13-524.

Scoma, S.R., Kubler, J., Nisumaa, A.M., 2016. The role of carbon concentrating mechanisms in the varied response of the green macroalga, *Ulva Lactuca*, to ocean acidification. Am. Geophys. Union EC54A-1312.

Shang, T., Lin, L., Chen, B., et al., 2020. Cell density-dependent suppression on the development and photosynthetic activities of *Sargassum fusiformis* embryos by

dinoflagellate *Karenia mikimotoi*. Harmful. Algae 96, 101842. https://doi.org/10.1016/j.hal.2020.101842.

Shimakawa, G., Murakami, A., Niwa, K., Matsuda, Y., Wada, A., Miyake, C., 2019. Comparative analysis of strategies to prepare electron sinks in aquatic photoautotrophs. Photosynth. Res. 139, 401–411. https://doi.org/10.1007/s11120-018-0522-z.

Singh, S.K., Sundaram, S., Sinha, S., Rahman, M.A., Kapur, S., 2016. Recent advances in CO_2 uptake and fixation mechanism of cyanobacteria and microalgae. Crit. Rev. Environ. Sci. Technol. 46, 1297–1323. https://doi.org/10.1080/10643389.2016.1217911.

Stitt, M., Krapp, A., 1999. The interaction between elevated carbon dioxide and nitrogen nutrition: the physiological and molecular backgroun. Plant Cell Environ. 22, 583–621. https://doi.org/10.1046/j.1365-3040.1999.00386.x.

Sun, J., Bao, M., Xu, T., Li, F., Wu, H., Li, X., Xu, J., 2021. Elevated CO_2 influences competition for growth, photosynthetic performance and biochemical composition in *Neopyropia yezoensis* and *Ulva prolifera*. Algal Res., (Amsterdam) 56, 102313. https://doi.org/10.1016/j.algal.2021.102313.

Sun, Y., Chen, X., Zhang, L., Liu, H., Liu, S., Yu, H., Wang, X., Qin, Y., Li, P., 2019. The antiviral property of *Sargassum fusiforme* polysaccharide for avian leukosis virus subgroup J in vitro and in vivo. Int. J. Biol. Macromol. 138, 70–78. https://doi.org/10.1016/j.ijbiomac2019.07.073.

Sun, Y., Zerges, W., 2015. Translational regulation in chloroplasts for development and homeostasis. Biochim. Biophys. Acta Bioenerg. 1847, 809–820. https://doi.org/10.1016/j.bbabio.2015.05.008.

Thangaraj, S., Sun, J., 2021. Transcriptomic reprogramming of the oceanic diatom *skeletonema dohrnii* under warming ocean and acidification. Environ. Microbiol. 23, 980–995. https://doi.org/10.1111/1462-2920.15248.

Tian, S., Chen, B., Wu, M., Cao, C., Gu, Z., Zheng, T., Zou, D., Ma, Z., 2022a. Are there environmental benefits derived from coastal aquaculture of *Sargassum fusiforme*? Aquaculture 562 (1), 738909.

Tian, S., Zheng, T., Wu, M., Cao, C., Xu, L., Gu, Z., Chen, B., Ma, Z., 2022b. Differences of photosynthesis and nutrient utilization in *Sargassum fusiforme* and its main epiphyte, *ulva lactuca*. Aquac. Res. 53 (8), 3176–3187. https://doi.org/10.1111/are.15830.

(University of Turku, Turku, Finland.) Tyystjarvi, E., Aro, E.M., 1996. The rate constant of photoinhibition, measured in lincomycin-treated leaves, is directly proportional to light intensity. Proc. Natl. Acad. Sci. – PNAS. 93, 2213–2218. https://doi.org/10.1073/pnas.93.5.2213.

Uddin, S., Löw, M., Parvin, S., Fitzgerald, G.J., Tausz-Posch, S., Armstrong, R., et al., 2018. Elevated [CO_2] mitigates the effect of surface drought by stimulating root growth to access sub-soil water. PLoS. One 13, e0198928. https://doi.org/10.1371/journal.pone.0198928.

Walters, K.A., Golbeck, J.H., 2018. Expression, purification and characterization of an active C491G variant of ferredoxin sulfite reductase from *synechococcus* elongatus PCC 7942. Biochim. Biophys. Acta (BBA)-Bioenerget. 1859, 1096–1107. https://doi.org/10.1016/j.bbabio.2018.06.014.

Wei, Z., Zhang, Y., Yang, F., Liang, J., Long, L., 2021. Increased light availability modulates carbon and nitrogen accumulation in the macroalga *Gracilariopsis lemaneiformis* (Rhodophyta) in response to ocean acidification. Environ. Exp. Bot. 187, 104492. https://doi.org/10.1016/j.envexpbot.2021.104492.

Wen, J., Zou, D., 2021. Interactive effects of increasing atmospheric CO_2 and copper exposure on the growth and photosynthesis in the young sporophytes of *Sargassum fusiforme* (Phaeophyta). Chemosphere (Oxford) 269, 129397. https://doi.org/10.1016/j.chemosphere.2020.129397.

Wu, Y., Gao, K., Riebesell, U., 2010. CO_2-induced seawater acidification affects physiological performance of the marine diatom *phaeodactylum tricornutum*. Biogeosciences. 7, 2915–2923. https://doi.org/10.5194/bg-7-2915-2010.

Vaish, S., Gupta, D., Mehrotra, R., Mehrotra, S., Basantani, M.K., 2020. Glutathione S-transferase: a versatile protein family. 3. Biotech. 10 (7), 321. https://doi.org/10.1007/s13205-020-02312-3.

Xu, L., Lin, L., Luo, L., Zuo, X., Cao, C., Jin, X., Jin, A., Ma, Z., Chen, B., Wu, M., 2022. Organic acid treatment for removal of epiphytic *ulva* L. attached to *Sargassum fusiforme* seedlings. Aquaculture 547, 737533. https://doi.org/10.1016/j.aquaculture.2021.737533.

Xu, Z., Zou, D., Gao, K., 2008. Effects of increased atmospheric CO_2 and N supply on growth, biochemical compositions and uptake of nutrients in *Gracilaria lemaneiformis* (Rhodophyta). Acta Ecol. Sin. 28, 3752–3759 (In Chinese with English abstract).

Xu, Z., Zou, D., Gao, K., 2010. Effects of elevated CO_2 and phosphorus supply on growth, photosynthesis and nutrient uptake in the marine macroalga *Gracilaria lemaneiformis* (Rhodophyta). Bot. Mar. 53, 123–129. https://doi.org/10.1515/BOT.2010.012.

Yadav, S., Mishra, A., 2020. Ectopic expression of C4 photosynthetic pathway genes improves carbon assimilation and alleviate stress tolerance for future climate change. Physiol. Mol. Biol. Plants. 26, 195–209. https://doi.org/10.1007/s12298-019-00751-8.

Yong, Y.S., Yong, W.T.L., Anton, A., 2013. Analysis of formulae for determination of seaweed growth rate. J. Appl. Phycol. 25, 1831–1834. https://doi.org/10.1007/s10811-013-0022-7.

Zemah-Shamir, S., Zemah-Shamir, Z., Tchetchik, A., Haim, A., Tchernov, D., Israel, Á., 2021. Cultivating marine macroalgae in CO_2-enriched seawater: a bio-economic approach. Aquaculture 544, 737042. https://doi.org/10.1016/j.aquaculture.2021.737042.

Zhang, R., Zhang, X., Tang, Y., Mao, J., 2020a. Composition, isolation, purification and biological activities of *Sargassum fusiforme* polysaccharides: a review. Carbohydr. Polym. 228, 115381. https://doi.org/10.1016/j.carbpol.2019.115381.

Zhang, X., Xu, D., Guan, Z., Wang, S., Zhang, Y., Wang, W., et al., 2020b. Elevated CO_2 concentrations promote growth and photosynthesis of the brown alga *Saccharina japonica*. J. Appl. Phycol. 32, 1949–1959. https://doi.org/10.1007/s10811-020-02108-1.

Zou, D., 2005. Effects of elevated atmospheric CO_2 on growth, photosynthesis and nitrogen metabolism in the economic brown seaweed, *Hizikia fusiforme* (*Sargassaceae*, Phaeophyta). Aquaculture 250, 726–735. https://doi.org/10.1016/j.aquaculture.2005.05.014.

Zou, D., Gao, K., Xia, J., 2003. Photosynthetic utilization of inorganic carbon in the economic brown alga, *hizikia fusiforme* (*Sargassaceae*) from the South China sea. J. Phycol. 39, 1095–1100. https://doi.org/10.1111/j.0022-3646.2003.03-038.x.